TKK Dissertations 117
Espoo 2008

STUDY OF CORTICAL RHYTHMIC ACTIVITY AND CONNECTIVITY WITH MAGNETOENCEPHALOGRAPHY

Doctoral Dissertation

Jan Kujala

Helsinki University of Technology
Faculty of Information and Natural Sciences
Department of Biomedical Engineering and Computational Science
Brain Research Unit, Low Temperature Laboratory

TKK Dissertations 117
Espoo 2008

STUDY OF CORTICAL RHYTHMIC ACTIVITY AND CONNECTIVITY WITH MAGNETOENCEPHALOGRAPHY

Doctoral Dissertation

Jan Kujala

Dissertation for the degree of Doctor of Science in Technology to be presented with due permission of the Faculty of Information and Natural Sciences for public examination and debate in Auditorium TU2 at Helsinki University of Technology (Espoo, Finland) on the 24th of April, 2008, at 12 noon.

Helsinki University of Technology
Faculty of Information and Natural Sciences
Department of Biomedical Engineering and Computational Science
Brain Research Unit, Low Temperature Laboratory

Teknillinen korkeakoulu
Informaatio- ja luonnontieteiden tiedekunta
Lääketieteellisen tekniikan ja laskennallisen tieteen laitos
Aivotutkimusyksikkö, Kylmälaboratorio

Distribution:
Helsinki University of Technology
Low Temperature Laboratory
P.O. Box 5100
FI - 02015 TKK
FINLAND
URL: http://ltl.tkk.fi/
Tel. +358-9-451 5619
Fax +358-9-451 2969
E-mail: jjkujala@neuro.hut.fi

ISBN 978-951-22-9339-1
ISBN 978-951-22-9340-7 (PDF)
ISSN 1795-2239
ISSN 1795-4584 (PDF)
URL: http://lib.tkk.fi/Diss/2008/isbn9789512293407/

TKK-DISS-2455

Picaset Oy
Helsinki 2008

ABSTRACT OF DOCTORAL DISSERTATION	HELSINKI UNIVERSITY OF TECHNOLOGY P.O. BOX 1000, FI-02015 TKK http://www.tkk.fi

Author Jan Kujala

Name of the dissertation
Study of cortical rhythmic activity and connectivity with magnetoencephalography

Manuscript submitted 11.01.2008	Manuscript revised 20.03.2008
Date of the defence 24.04.2008	
☐ Monograph	☒ Article dissertation (summary + original articles)

Faculty	Faculty of Information and Natural Sciences
Department	Department of Biomedical Engineering and Computational Science
Field of research	Neuroscience
Opponent(s)	Dr. Stefan Kiebel
Supervisor	Prof. Risto Ilmoniemi
Instructor	Acad. Prof. Riitta Salmelin

Abstract

Intracranial recordings in animals and neuroimaging studies on humans have indicated that oscillatory activity and its modulations may play a fundamental role in large-scale neural information processing. Furthermore, rhythmic interactions between cortical areas have been detected across a variety of tasks with electroencephalography (EEG) and magnetoencephalography (MEG). This kind of coupling has been proposed to be a key mechanism through which information is integrated across segregated areas. So far, rhythmic interactions have been analyzed primarily at the EEG/MEG sensor level, without explicit knowledge of cortical areas involved.

In this thesis work we developed new methods that can be used to image oscillatory activity and coherence at the cortical level with MEG. Dynamic Imaging of Coherent Sources (DICS) enables localization of interacting areas both using external reference signals and directly from the MEG data. When the interacting areas have been determined it is possible to use additional measures beyond coherence to further quantify interactions within the networks. DICS was originally designed for study of continuous data; its further development into event-related DICS (erDICS) adds the possibility to image modulations of rhythmic activity that are locked to stimulus or movement timing. Furthermore, permutation testing incorporated into erDICS allows the evaluation of the statistical significance of the results. Analysis of simulated and real data showed that DICS and erDICS yield accurate localization and quantification of oscillatory activity and coherence. Comparison of DICS to other methods of localizing oscillatory activity revealed that it is equally accurate and that it can better separate the activity originating from two nearby areas.

We applied DICS to two datasets, recorded from groups of subjects while they performed slow finger movements and when they were reading continuously. In both cases, we were able to systematically identify interacting cortico-cortical networks and, using phase coupling and causality measures, to quantify the manner in which the nodes within these networks influenced each other. Furthermore, we compared the identified reading network to results reported in neurophysiological and hemodynamic activation studies. In addition to areas typically detected in activation studies of reading the network included areas that are normally found in language production rather than perception tasks, indicating more extensive networking of neural systems than usually observed in activation studies.

Keywords magnetoencephalography, beamforming, rhythmic activity, cortical interactions, coherence

ISBN (printed) 978-951-22-9339-1	ISSN (printed) 1795-2239
ISBN (pdf) 978-951-22-9340-7	ISSN (pdf) 1795-4584
Language English	Number of pages 67 p. + app. 82 p.

Publisher Low Temperature Laboratory, Helsinki University of Technology

Print distribution Low Temperature Laboratory, Helsinki University of Technology

☒ The dissertation can be read at http://lib.tkk.fi/Diss/2008/isbn9789512293407/

VÄITÖSKIRJAN TIIVISTELMÄ	TEKNILLINEN KORKEAKOULU PL 1000, 02015 TKK http://www.tkk.fi

Tekijä Jan Kujala

Väitöskirjan nimi
Kortikaalisen rytmisen toiminnan ja kytkeytyvyyden tutkiminen magnetoenkefalografialla

Käsikirjoituksen päivämäärä 11.01.2008	Korjatun käsikirjoituksen päivämäärä 20.03.2008

Väitöstilaisuuden ajankohta 24.04.2008

☐ Monografia	☒ Yhdistelmäväitöskirja (yhteenveto + erillisartikkelit)

Tiedekunta	Informaatio- ja luonnontieteiden tiedekunta
Laitos	Lääketieteellisen tekniikan ja laskennallisen tieteen laitos
Tutkimusala	Neurotiede
Vastaväittäjä(t)	Dr. Stefan Kiebel
Työn valvoja	prof. Risto Ilmoniemi
Työn ohjaaja	akat. prof. Riitta Salmelin

Tiivistelmä

Suoraan aivojen sisältä tehtävät mittaukset eläimillä ja kuvantamistutkimukset ihmisillä ovat antaneet viitteitä siitä, että aivojen rytmisellä toiminnalla ja sen muutoksilla saattaa olla oleellinen rooli aivojen tiedonkäsittelyssä. Lisäksi aivoalueiden välisiä rytmisiä vuorovaikutuksia on havaittu useissa eri tehtävissä elektroenkefalografialla (EEG) ja magnetoenkefalografialla (MEG). Tällaisen kytkeytyvyyden on ehdotettu olevan yksi avainmekanismeista, joilla tietoa yhdistetään eri aivoalueiden välillä. Toistaiseksi rytmisiä vuorovaikutuksia on tutkittu EEG:llä ja MEG:llä lähinnä anturien tasolla ilman, että näihin vuorovaikutuksiin osallistuvia aivoalueita olisi paikannettu.

Tässä väitöskirjatyössä kehitimme uusia menetelmiä, joita voidaan käyttää MEG:llä mitatun rytmisen toiminnan ja koherenssin kuvantamiseen aivojen tasolla. Dynamic Imaging of Coherent Sources (DICS) mahdollistaa vuorovaikuttavien alueiden paikannuksen sekä ulkoisia verrokkisignaaleja käyttäen että suoraan MEG:llä mitatusta datasta. Kun verkkojen solmukohdat on paikannettu, niiden väliset vuorovaikutukset voidaan määrittää myös koherenssia monitahoisemmilla mittayksiköillä. DICS suunniteltiin alunperin jatkuvan datan analysointiin; menetelmän uudemman muunnelman, event-related DICS:n (erDICS) avulla voidaan kuvantaa myös yksittäisiin tapahtumiin liittyvät rytmisen toiminnan muutokset. erDICS:illa voidaan lisäksi arvioida tulosten tilastollista merkittävyyttä permutaatiotestausta käyttäen. Simuloidun ja oikean MEG-datan analyysit osoittivat, että DICS ja erDICS paikantavat ja määrittävät rytmisen toiminnan ja koherenssin tarkasti. Kun vertasimme DICS:iä muihin rytmisen toiminnan paikannusmenetelmiin, havaitsimme, että se tuottaa yhtä tarkkoja tuloksia ja pystyy jopa paremmin erottamaan toisiaan lähellä olevien alueiden aktiivisuuden.

Sovelsimme DICS:iä kahteen datasarjaan, joista ensimmäisessä tutkittavat tekivät sormenliiketehtävää ja toisessa lukivat jatkuvaa tekstiä. Pystyimme molemmissa tapauksissa systemaattisesti tunnistamaan vuorovaikuttavat aivoverkot sekä käyttämällä vaihelukkiutuvuus- ja kausaliteettimittoja määrittämään näiden verkkojen solmukohtien vaikutukset toisiinsa. Vertasimme lisäksi lukemistehtävässä tunnistettua verkkoa aiempien aktivaatiotutkimusten antamiin tuloksiin. Verkko sisälsi tyypillisesti lukemistehtävissä tunnistettujen aivoalueiden lisäksi esimerkiksi alueita, jotka aktivoituvat pikemminkin kielen tuottossa kuin sen havaitsemisessa. Vuorovaikutusten kuvantamisen perusteella näyttää siis siltä, että kielen käsittelyyn osallistuu aivoissa paljon laajempia verkostoja kuin mitä voisi päätellä vain aktivaatiotutkimusten pohjalta.

Asiasanat magnetoenkefalografia, spatiaalien suodatus, rytminen toiminta, kortikaaliset vuorovaikutukset, koherenssi

ISBN (painettu) 978-951-22-9339-1	ISSN (painettu) 1795-2239
ISBN (pdf) 978-951-22-9340-7	ISSN (pdf) 1795-4584
Kieli englanti	Sivumäärä 67 s. + liit.82 s.

Julkaisija Kylmälaboratorio, Teknillinen korkeakoulu

Painetun väitöskirjan jakelu Kylmälaboratorio, Teknillinen korkeakoulu

☒ Luettavissa verkossa osoitteessa http://lib.tkk.fi/Diss/2008/isbn9789512293407/

Academic dissertation

Study of cortical rhythmic activity and connectivity with magnetoencephalography

Author:	Jan Kujala Brain Research Unit, Low Temperature Laboratory Helsinki University of Technology Finland
Supervising professor:	Prof. Risto Ilmoniemi Department of Biomedical Engineering and Computational Science Helsinki University of Technology Finland
Supervisor:	Acad. Prof. Riitta Salmelin Brain Research Unit, Low Temperature Laboratory Helsinki University of Technology Finland
Preliminary examiners:	Doc. Jukka Nenonen Elekta Neuromag Oy Helsinki, Finland Dr. Vadim Nikulin Charité University Medicine Berlin Germany
Official opponent:	Dr. Stefan Kiebel Wellcome Trust Centre for Neuroimaging Institute of Neurology, UCL United Kingdom

Table of contents

List of publications

P1 Gross J, **Kujala J**, Hämäläinen M, Timmermann L, Schnitzler A, Salmelin R. Dynamic imaging of coherent sources: Studying neural interactions in the human brain. PNAS 2001; 98: 694–699.

P2 Gross J, Timmermann L, **Kujala J**, Dirks M, Schmitz F, Salmelin R, Schnitzler A. The neural basis of intermittent motor control in humans. PNAS 2002; 99: 2299–2302.

P3 Gross J, Timmermann L, **Kujala J**, Salmelin R, Schnitzler A. Properties of MEG tomographic maps obtained with spatial filtering. Neuroimage 2003; 19: 1329–1336.

P4 Liljeström M, **Kujala J**, Jensen O, Salmelin R. Neuromagnetic localization of rhythmic activity in the human brain: a comparison of three methods. Neuroimage 2005; 25: 734–745.

P5 **Kujala J**, Pammer K, Cornelissen PL, Roebroeck A, Formisano E, Salmelin R. Phase coupling in a cerebro-cerebellar network at 8-13 Hz during reading. Cerebral Cortex 2007; 17: 1476–1485.

P6 Salmelin R, **Kujala J**. Neural representation of language: activation versus long-range connectivity. Trends in Cognitive Sciences 2006; 10: 519–525.

P7 **Kujala J**, Gross J, Salmelin R. Localization of correlated network activity at the cortical level with MEG. Neuroimage 2008; 39; 1706–1720.

P8 Laaksonen H, **Kujala J**, Salmelin R. A method for spatiotemporal mapping of event-related modulation of cortical rhythmic activity. TKK Report, TKK-KYL-019.

Contributions of the author

All publications included in this thesis are a result of group effort. I was the principal investigator and author in studies P5 and P7, and contributed actively to the writing of publications P1-P4, P6 and P8. In P5, I developed and implemented the necessary analysis tools and carried out the data analysis, and I actively participated in the experimental design and data collection. In P7, I designed and constructed the simulations needed for testing the method and analyzed the simulated and measured data sets. I was responsible for connectivity analysis of the data presented in P6. In P1-P4 and P8 I was keenly involved in construction of the simulations and in the development and implementation of the analysis tools and, in P4 and P8, in the practical data analysis.

Abbreviations

BEM	Boundary Element Method
BOLD	Blood Oxygen Level Dependent
CSD	Cross-Spectral Density
DCM	Dynamic Causal Modeling
DI	Directionality Index
DICS	Dynamic Imaging of Coherent Sources
DTF	Directed Transfer Function
DTI	Diffusion Tensor Imaging
ECD	Equivalent Current Dipole
EEG	Electroencephalography
EMG	Electromyogram
EOG	Electro-oculogram
ERD	Event-Related Desynchronization
erDICS	event-related Dynamic Imaging of Coherent Sources
ERS	Event-Related Synchronization
FFT	Fast Fourier Transform
fMRI	functional Magnetic Resonance Imaging
FWHM	Full Width at Half Maximum
LFP	Local Field Potential
M1	Primary Motor Cortex
MCE	Minimum Current Estimate
MEG	Magnetoencephalography
MFT	Magnetic Field Tomography
MNE	Minimum Norm Estimate
MRI	Magnetic Resonance Imaging
PDC	Partial Directed Coherence
PET	Positron Emission Tomography
PLV	Phase-Locking Value
PLS	Phase-Locking Statistics
PMC	Premotor Cortex
ROI	Region Of Interest
RSVP	Rapid Serial Visual Presentation
SEM	Structural Equation Modeling
SI	Synchronization Index
SQUID	Superconducting Quantum Interference Device
SNR	Signal-to-Noise Ratio
SSS	Signal Space Separation
TMS	Transcranial Magnetic Stimulation

Preface and acknowledgements

This thesis work was carried out in the Brain Research Unit of the Low Temperature Laboratory at the Helsinki University of Technology, and it would not have been possible to complete the work without the contribution of professors Mikko Paalanen and Riitta Hari, the heads of the Low Temperature Laboratory and the Brain Research Unit. Their continuous efforts and hard work have generated an excellent and productive research environment, and ensured that all the best resources and toys, i.e., multimillion-euro neuroimaging devices, have been available. Regarding the resources required for completing this thesis, I am also grateful to the Finnish Graduate School of Neuroscience, the James S. McDonnell Foundation 21st Century Research Award, the Academy of Finland, and the Sigrid Jusélius Foundation for funding this work.

The greatest debt for ever finishing thesis I owe to my supervisor, Acad. Prof. Riitta Salmelin. She has provided all the possible motivation, guidance and support, along every step of the way, enabling me to reach this goal that often seemed so very far away. For that, I am grateful beyond words. She has always taken the time and effort to discuss, comment and encourage. I have never felt left alone to perform the research and despair; I have known from start to finish that completing this thesis is our common goal, with both of us doing our best to reach the end.

I would also like to thank my supervising Prof. Risto Ilmoniemi. Although we came to contact quite late in this thesis work, his insightful comments helped me clarify the summary of this thesis work, and his help in the last steps was paramount. I am also very grateful to the preliminary examiners Doc. Jukka Nenonen and Dr. Vadim Nikulin for their comments that made it possible for me to tune this thesis into a much more elegant version than what I would have managed on my own. I would also like to thank Doc. Jukka Nenonen and Dr. Antti Tarkiainen for their guidance as the members of my Finnish Graduate School of Neuroscience follow-up group; I very much appreciated the meetings we had, and the feeling that there were people in the world who understood the woes of my thesis work. I am also grateful to Dr. Cathy Nangini for honing the language of this thesis into actual English, and also for helping me ascertain that the summary can be understood by people not involved in the writing process.

Furthermore, although this is my thesis of which I am solely responsible, I by no means did all the work, and certainly not alone. I am forever grateful to all my collaborators, for their contribution and for their company. Foremost, I would like to thank Prof. Joachim Gross, the mastermind behind the main methodology. His brilliant and precise mind laid a foundation for this work that has supported it throughout the years. I would also like to express my heartfelt gratitude to all my other co-authors, both near and far away: Ms. Mia Liljeström, Mr. Hannu Laaksonen, Prof. Matti Hämäläinen, Dr. Ole Jensen, Prof. Alfons Schnitzler, Dr. Lars Timmermann, Dr. Martin Dirks, Dr. Frank Schmitz, Dr. Kristen Pammer, Dr. Piers Cornelissen, Dr. Alard Roebroeck, and Dr. Elia Formisano. And, although their scientific contribution did not manifest itself as a co-

authorship, I would like to thank Dr. Kimmo Uutela for solving the forward problem, Dr. Mika Seppä for the most beneficial deformations, and Mr. Lauri Parkkonen for unveiling the mysteries of MEG.

I am also grateful to all the people in the Laboratory, particularly the senior scientists, Doc. Päivi Helenius, Doc. Veikko Jousmäki, Doc. Simo Vanni, and Doc. Nina Forss, for their direct and indirect contributions that have helped me over the years. I would also like to thank the administrative staff of the laboratory, Pirjo Kinanen, Liisi Pasanen, Tuire Koivisto, Teija Halme, Satu Pakarinen, and Leena Meilahti for taking care of all the arrangements, were they regarding my salary, my travel invoices or the shopping bills I left at their door.

Of the people of the laboratory, I would like to above all thank the people of Siberia, especially those who inhabited its South Wing with me, for their company and friendship over the years. Antti Tarkiainen, Cristina Simões and Gina Caetano; Obrigado. Although the walls of Siberia have been torn down, I will never forget the years I spent there or the good people of Siberia. Moreover, the positive side of spending more than the optimum of four years on this thesis enabled me to get to know many fine individuals much better than I would have in the "optimal" case. I have really appreciated sharing both the good and the bad with Tiina Parviainen, Hanna Renvall and Topi Tanskanen. And as for time spent, had I spent all that time alone in the "Server Room" and on related tasks, I might never have risen from that abyss. Mika, thank you for sharing the pain.

I would also like to express my appreciation to all the people in BRU, past and present, plus a few associated people, for their companionship, and for assorted more and less work related things. In alphabetical order, disbarring dyslexia: Maarit Aro, Paolo Belardinelli, Milene Bonte, Samuli Hakala, Marja-Liisa Halko, Liisa Helle, Linda Henriksson, Jaana Hiltunen, Lotta Hirvenkari, Yevhen Hlushchuk, Annika Hultén, Mia Ilman, Antti Jalava, Juha Järveläinen, Jaakko Järvinen, Helge Kainulainen, Jari Kainulainen, Marita Kattelus, Erika Kirveskari, Satu Lamminmäki, Marieke Longcamp, Sanna Malinen, Elina Pihko, Marjatta Pohja, Tuukka Raij, Pavan Rankumar, Ville Renvall, Petteri Räisänen, Timo Saarinen, Veli-Matti Saarinen, Ronny Schreiber, Martin Schürmann, Sini Sipponen, Päivi Sivonen, Linda Stenbacka, Oguz Tanzer, Samu Taulu, Johanna Vartiainen, Nuutti Vartiainen, Ricardo Vigario, Minna Vihla, and Katri Wegelius.

Regarding the life out of science, I would like to thank all my friends and my family, for providing me with an actual life and thus preventing the world from ending with the bad review comments. In particular, I thank Juha Riikonen and Jere Knuuttila for the truly cross-scientific symposia we had over the years and for the invaluable perspective these meetings provided. I would also like to thank all the boys of the Tuesday sähly for the most essential hour of the working week. Moreover, I am especially grateful to Marja-Leena, Matti and Santtu Saarela for the home away from home where I have managed to regain the strength lost along the way. And, needless to say, why it has remained mostly unsaid, I am extremely grateful to my parents Eija and Jaakko for all their emotional, spiritual and financial support that have been fundamental in so much along the entire path of my life.

Last. And most. I would like to thank you Miiu for making the last years, as arduous as they have sometimes been, by far the best of my life. This thesis work would probably have been finished without you, but so would I. To you, I owe my life and my happiness, now, and in the years to come.

Espoo, April 2008

Jan Kujala

1 Introduction

1.1 Background

The brain can process information entering via the sensory organs and, also, give rise to intricate functioning that links directly to behavior. All this is based on electric currents and chemical reactions taking place in neurons, cells specialized in receiving and transmitting signals within the brain, and between the brain and the rest of the body. The properties and functions of neurons have been studied extensively both at the level of individual neurons and their sub-cellular elements, and at the level of networks of neurons forming larger assemblies. Yet, it is still unclear how the brain is able to, e.g., integrate the vast amount of neuronal processes into one percept, or how this percept affects the subsequent changes in attention towards the most relevant input (La Berge, 1995; Büchel and Friston, 1997; Singer, 1999).

It has been suggested that integration of information does not take place through neurons and brain areas related to individual functions working in isolation, but through interaction of spatially segregated neuronal assemblies (Mesulam, 1990; Varela et al., 2001). Two mechanisms have been suggested to support exchange of information between cortical areas: stimulus-induced coordination and internally generated synchronization (Singer, 1999). The main concept in stimulus-induced coordination is that information proceeds hierarchically and sequentially via the cortical areas. Formation of a cognitive percept from sensory input would occur through integration of information in associative areas. In integration of information through internally generated synchronization, dynamical interaction between areas would generate the single percept. Alternatively, it may be that part of the information exchange is hierarchical, either feed-forward or feed-back, but that parts of the large-scale neuronal networks interact through reciprocal connectivity between areas.

For the reciprocal interactions, modulation and coupling of rhythmic activity at the level of large-scale cortical networks have been proposed to be the mechanisms through which information and influence are transmitted (Classen et al., 1998; Singer, 1999; von der Malsburg, 1999; Pfurtscheller et al., 2000; Varela et al., 2001). First, it has been hypothesized that low-frequency oscillations can maintain information available for longer periods than stimulus-evoked transient activity, which could be beneficial for combining information between sequential events (Dinse et al., 1997). Second, phase synchronization between neuronal groups has been proposed to be the mechanism through which integration of information takes place (Varela et al., 2001).

Taken together, the ability to identify the generators of rhythmic activity and detect their mutual coupling should enable characterization of integrative information processing in the brain. These types of investigations are possible to perform non-invasively at the neuronal population level with functional neuroimaging techniques. Neurophysiological imaging techniques, magnetoencephalography (MEG) and electroencephalography (EEG), record directly the fields generated by neural activity. However, because of the nature of electromagnetic fields, it is not possible to

unequivocally determine the cortical sources from the MEG and EEG recordings (Helmholz, 1853), unless one makes some assumptions about the sources or sets constraints on the solution (Hämäläinen et al., 1993; Baillet et al., 2001). Hence, many neurophysiological analyses have been performed at the EEG/MEG sensor level, without explicitly localizing the cortical areas involved in the studied task. Secondly, hemodynamic imaging techniques, functional magnetic resonance imaging (fMRI) and positron emission tomography (PET), record changes in cerebral blood flow and oxygen consumption. Although these techniques do not reveal directly the underlying neuronal activity, and although the exact relationship between neuronal activity and the ensuing metabolic changes is unclear, the great benefit of hemodynamic imaging techniques is that they yield a univocal, high-resolution spatial estimate of active brain areas.

1.2 Aim and outline of the thesis

At the start of this thesis work, due to lack of suitable analysis tools, large-scale neural information processing via cortical rhythmic activity and particularly via rhythmic interactions between cortical areas had been investigated primarily at the MEG/EEG sensor level, without explicitly identifying the brain areas involved. This thesis work focuses on development of a new analysis method for MEG data, Dynamic Imaging of Coherent Sources (DICS), which allows the study of neuronal activity as reflected in the amount of oscillatory power and in the long-range interactions of oscillatory components at the cortical level. DICS is well suited for analysis of continuous, non-averaged data and, thus, facilitates the use of increasingly natural experimental designs. We also applied DICS to two recorded datasets to explicitly determine the cortical origins of rhythmic interactions during motor performance and language processing, and to quantify the mutual interactions between the nodes of the identified networks.

Chapter 2 of this thesis portrays processing and exchange of information at the neuronal population level, based on data recorded in animals and humans. The chapter describes various measures of cortico-cortical activity and coupling, techniques for studying them and results obtained with these techniques. Chapter 3 outlines the basis of MEG and how it can be used to record neuronal activity from the human brain, and recounts different approaches for estimating activity at the cortical level from data recorded by MEG sensors.

Chapter 4 describes the methodological development done in this thesis work, specifically the basis of DICS and how it can be used to obtain estimates of oscillatory activity and interareal coherence in the human brain. I will show that DICS provides valid estimates of oscillatory power and coherence, both for simulated and real data. I will consider the properties of these estimates in different parts of the cortex and at different levels of noise. Furthermore, I will compare the localization of oscillatory power with DICS to results obtained with other analysis tools, and show that results obtained with DICS are comparable to, and in some cases, more sensitive than those obtained with other analysis tools. I will also present a modification of DICS, event-related Dynamic Imaging of Coherent Sources (erDICS), which is a technique suitable for localizing event-related modulation of rhythmic activity. erDICS also incorporates

permutation testing which enables evaluation of the statistical significance of the findings in individual subjects. In the last part of the chapter, I will demonstrate how cortico-cortical networks can be identified using various approaches for localizing cortical reference areas, and how different parameters and intersubject variability affect the accuracy of DICS interaction analysis.

Chapter 5 details two studies, in which DICS was applied to real data recorded from a group of subjects, and presents the identified interacting cortico-cortical networks. In the first study, DICS was used to identify an interacting motor network during a finger movement task. Phase coupling and causal interaction measures were applied to show that it is possible not only to identify the relevant areas, but also to characterize the degree in which they interact and the manner in which they influence each other. In the second study, DICS was used to localize cortico-cortical networks during continuous reading. The subsequent phase coupling and causality analysis demonstrated that these areas interacted systematically across individuals during the tasks. In the last part of the chapter, I will compare the identified interacting cortical network in reading to localization results obtained from various neurophysiological and hemodynamic activation studies of language function, and argue that together these approaches importantly extend our knowledge of language processing.

In conclusion, I will consider the relevance of these studies in a larger perspective and the limitations of the approaches used in these studies. Furthermore, I will discuss directions that need to be taken in methodological development and application of the methods to real recorded data in order to obtain a more complete picture of cortical information processing.

2 Large-scale neural information processing

For almost a century, it has been possible to record population-level electric neuronal activity from the human brain. These neurophysiological studies have mainly focused on cortical information processing during stimulus-induced activation, in terms of so-called evoked responses and event-related modulation of rhythmic activity. In addition, spontaneous rhythmic activity has been studied in healthy and pathological conditions. Analyses have been performed either on the signals recorded from outside the head or by first estimating the sources of neural activity at the cortical level. Recently, interactions between cortical regions have been analyzed to characterize interareal information transfer, as opposed to making hypotheses based on the sequence and modulation of activity at different sites. In animal studies, intracranial recordings have yielded evidence of interactions between different functional areas, typically within relatively small patches of cortex. In human studies, however, such recordings have been restricted to patients. Systematic analysis of neural interactions in the healthy human brain has thus been performed mostly on the EEG/MEG sensor level, without explicitly identifying the underlying cortical areas. In addition, hemodynamic neuroimaging techniques have been applied in evaluating connectivity between brain regions. Although the identification of cortical areas is explicit in these methods, the indirect relationship between the recorded signals and neural activity limits the amount of information that can be obtained regarding neural processes. Furthermore, during the last decade, the development of diffusion tensor imaging (DTI) has made it possible to obtain information about anatomical connections between cortical areas in the working human brain and, thus, to map routes through which information can be transferred between cortical areas.

2.1 Evoked neurophysiological responses

In neurophysiological recordings, the most frequently used measure of large-scale neuronal processes is the stimulus-induced evoked response. Neural signals, generated by external stimuli or events, propagate through different brain regions. This information flow in the brain, at the neuronal population level, can be followed by recording the ensuing electric or magnetic signals with EEG or MEG. In evoked response analysis, tens to hundreds of events are typically recorded and averaged in order to improve the signal-to-noise ratio (SNR). The underlying assumption is that the neural response occurs similarly from trial to trial, phase-locked to the stimulus, and that the background noise is uncorrelated across trials. There are two main theories as to how the evoked responses are generated in neural populations. The first theory, referred to as either the additive model or amplitude modulation, states that the evoked responses are generated by transient brain events which do not affect the ongoing oscillatory activity (Penny et al., 2002; Shah et al., 2004; Mazaheri and Jensen, 2006). In this model, the spontaneous oscillatory activity is largely irrelevant with regard to the evoked responses. However, evidence also exists that partial phase resetting of ongoing

oscillations can give rise to evoked responses (Makeig et al., 2002; Penny et al., 2002). According to the proposed phase resetting model, evoked responses arise from alignment of phases of ongoing background oscillations to the stimulus, resulting in the emergence of the event-related response in the averaged data.

In MEG, evoked responses have been traditionally applied to study of sensory events, e.g., in the visual (Brenner et al., 1975), somatosensory (Brenner et al., 1978) and auditory (Hari et al., 1980) modalities. Brain function has been evaluated in this manner also in more complex tasks such as picture naming (Salmelin et al., 1994) and sentence comprehension (Helenius et al., 1998). A key element is to vary the stimuli parametrically, along one dimension at a time. Thus, differences in the responses between conditions should, ideally, indicate that certain types of information are processed in certain cortical areas and time windows. Moreover, in MEG the combination of reasonably good localization and millisecond scale temporal resolution enables identification of different routes of information processing in the brain, such as separate streams for processing spatial and phonetic changes in the human auditory system (Ahveninen et al., 2006).

2.2 Rhythmic activity in the brain

The first EEG recordings revealed oscillatory activity arising from the human brain (Berger, 1929). Subsequently, rhythmic activity has been classified into specific components based on the frequency content and spatial distribution of the oscillations. The best known components are the posterior alpha (8-13 Hz) and rolandic mu (comb-like shape, 7-13 and 16-24 Hz) rhythms (Berger, 1929; Gastaut, 1952). Although these rhythms are often called spontaneous, it has been shown that external events, movements or the level of arousal, may affect them (Berger, 1930; Chatrian et al., 1959; Hari and Salmelin, 1997). In addition to alpha and mu, typical oscillatory components include theta (3-8 Hz) and beta (13-30 Hz) rhythms, originating typically from frontal and somatomotor cortices, respectively (Hari and Salmelin, 1997; Ishii et al., 1999). Gamma band activity (30-100 Hz), in turn, has been reported in multiple cortical areas (Singer, 1993; Tallon-Baudry et al., 1997). Moreover, neurological disorders are often accompanied by marked changes in the spectral composition and overall level of rhythmic activity as compared with the normal pattern (Gloor et al., 1977; Aminoff, 1986; Mäkelä et al., 1993).

From the information processing point of view, perhaps more relevant than the location of different rhythms and their changes in neurological disorders is the fact that the cortical rhythms can also be modulated transiently by tasks and stimuli. This modulation can take two forms, often referred to as event-related synchronization (ERS) and desynchronization (ERD) (Pfurtscheller, 1977, 1992; Pfurtscheller and Lopes da Silva, 1999). The two types of modulations can occur in combination, i.e., an initial suppression is followed by a strong rebound above the base-level of rhythmic activity (Salmelin and Hari, 1994b). Compared to evoked responses, the critical difference in both ERS and ERD is that they are not typically phase-locked to the stimuli. Accordingly, they disappear in direct averaging. Instead, estimates of the event-related modulations of rhythmic activity can be obtained by first calculating for each

event the power at the frequency of interest, and then averaging those values across trials. As the event-related modulation of rhythmic activity and evoked responses lock differently to external events, it may be that there is something fundamentally different in their mechanisms and, thus, possibly in their roles in information processing and transfer in the brain.

The non-phase-locked modulation of rhythmic activity has been studied in multiple tasks both with EEG and MEG, using various methods that quantify the amplitude or power of the responses. Historically, the best known modulations are suppressions and enhancements related to movement and somatosensory input. For example, suppression of the rolandic 10- and 20-Hz components has been detected for both somatosensory stimulation and preparation for movement (Chatrian et al., 1959). After voluntary movement there is first a suppression of rhythmic activity, followed by a return to normal level in a couple of seconds after the movement (Penfield, 1954; Chatrian et al., 1959; Pfurtscheller, 1981). MEG recordings have shown that the post-movement 20-Hz rebound occurs 300 ms earlier than the rebound of 10-Hz rhythm, and that the 10-Hz component originates close to the hand somatosensory cortex whereas the generators of the 20-Hz component track the moving body part along the motor cortex (Salmelin and Hari, 1994b; Salmelin et al., 1995). These findings would suggest that the 10-Hz signal largely reflects activity in the somatosensory cortex and the 20-Hz component primarily that of the motor cortex. It has also been shown that there are bursts of beta band activity in the hand motor region and bursts of activity at higher frequencies in the neighboring regions after ending a finger movement (Pfurtscheller et al., 2000). Event-related suppression of rhythmic activity has also been detected in other sensory modalities. For example, both visual recall and imagery are accompanied by a suppression of alpha rhythm in the parieto-occipital areas (Kaufman et al., 1990; Salenius et al., 1995), but 10- and 20-Hz components show distinct behavior in visual stimulation (Salmelin and Hari, 1994a). Furthermore, event-related suppression of 8-10-Hz activity (‘tau’ rhythm) has been detected in the temporal cortex during auditory stimulation (Tiihonen et al., 1991).

Event-related modulation of rhythmic activity has also been investigated in more complex tasks. When speech production was compared to non-speech mouth movements with similar kinetic properties, speech production was found to elicit more specific activation of the mouth motor cortex, as represented by the modulation of the 20-Hz rhythm (Saarinen et al., 2006). It has been shown that both alpha and theta band activity increase during retention in working memory, and that theta band activity increases during mental tasks (Ishii et al., 1999; Jensen et al., 2002; Jensen and Tesche, 2002). However, alpha band activity may also be suppressed during retention, as demonstrated in an investigation of a delayed double-step saccade task (Medendorp et al., 2006). Event-related changes in the gamma band have also been observed with EEG and MEG. For example, visual search was shown to elicit both phase-locked and non-phase-locked gamma-band oscillations, where only the later non-phase-locked activity reacted differently to target than nontarget stimuli (Tallon-Baudry et al., 1997). In addition, differences in gamma-band activity were detected in perception of illusory vs. real triangles (Kaiser et al., 2004), and stronger gamma-band responses to remembered items vs. forgotten ones in a declarative memory task (Osipova et al., 2006).

Thus, information processing that is not strictly phase-locked to the external stimuli can be followed by tracking changes of rhythmic activity that may subserve various functions in the brain. Furthermore, regarding the role of the various rhythms, it has been suggested that the extended temporal range of low-frequency cortical oscillations could be useful for combining information between temporally differentiated events, possibly across multiple cortical areas (Dinse et al., 1997). It must be noted, however, that many cortical rhythms are partially overlapping, both in frequency and in space. Thus, considering the large inter-individual variation in rhythmic activity (Steriade et al., 1990), the rhythms need to be characterized carefully with respect to both their spatial properties and their frequency content. In this endeavour, we need analysis methods that help us determine accurately the cortical origin of the rhythms, their frequencies and temporal behavior, as well as their task and stimulus dependence.

2.3 Coupling of neural activity

Evoked responses and modulation of rhythmic activity yield information on sequential processing of information occurring in the brain. It has been strongly advocated that in order for cognition to emerge, large-scale integration across cortical areas is required, whether one defines cognition as a cognitive moment or the resolving of a cognitive problem (Mesulam, 1990; Varela et al., 2001). In addition, it has been proposed that internal coordination of distributed responses is equally important and temporally as accurate as stimulus-induced coordination (Singer, 1999). Taken together, these two aspects would indicate that in order to understand how the brain handles information, we must be able to evaluate the cortico-cortical interaction of neuronal processes. Regarding these interactions, synchronization of oscillatory activity has been suggested to be the most likely candidate mechanism for linking spatially segregated areas and processes (Singer and Gray, 1995; Varela et al., 2001). Over the last 20 years, evidence from both intracranial recordings and neuroimaging studies has started to accumulate on how different brain areas interact and how such interactions are modulated by, e.g., external stimuli and attention.

2.3.1 Measures of neural coupling

Multiple measures have been suggested for quantifying interactions between neural populations. Coherence, which is still the most frequently applied measure of interaction, is calculated by first estimating the power spectral densities (P_{xx}, P_{yy}) for two signals (x, y) by averaging the squared magnitudes of their segment-wise Discrete Fourier Transforms (DFT). The cross spectral density (P_{xy}) is computed by multiplying and averaging the segment-wise DFTs of x and y. Coherence (C_{xy}) is then obtained as:

$$C_{xy} = \frac{\left|P_{xy}\right|^2}{P_{xx}P_{yy}}. \qquad (2.1)$$

Coherence is influenced by random fluctuations in the level of oscillatory activity. That is, even if the phases of the oscillators were perfectly matched, coherence could yield a low estimate for their mutual interaction. Accordingly, measures that are independent of the amplitudes of the signals may be more appropriate for describing synchronization between oscillators (Tass et al., 1998; Lachaux et al., 1999). Phase-locking value (PLV) is calculated by first estimating the instantaneous phase of signals at target frequency (Lachaux et al., 1999). This is accomplished by band-passing the signals and convolving them with a complex Gabor wavelet centered at the frequency of interest. PLV can then be calculated at time *t* as:

$$\mathrm{PLV}(t) = \frac{1}{N}\sum_{n=1}^{N} \exp(j(\theta(t, n)), \tag{2.2}$$

where $\theta(t, n)$ is the phase difference between the two signals for trial *n*. Thus, if the phase difference between the two signals remains relatively constant, PLV is close to 1. Phase-locking statistics (PLS) estimates the statistical significance of PLV. Here, the trial-order of one signal is shuffled (e.g. 1000 times) to obtain surrogate data. The phase-locking value is then calculated between the surrogate data and the second signal to obtain an estimate of whether the signals are phase-locked to the stimulus onset or to each other. Another phase-coupling measure, the synchronization index (SI), is applicable also to noisy and chaotic systems, and to both continuous and event-related tasks (Tass et al., 1998). SI is calculated by first estimating the instantaneous phases ($\phi_{1,2}$) of two signals using the Hilbert Transform, and by quantifying their relative phase ($\omega_{n,m}$) as:

$$\omega_{n,m}(t) = n\phi_1(t) - m\phi_2(t), \tag{2.3}$$

where *n* and *m* are integers and $\phi_{1,2}$ are normalized (divided by 2π) phases of the two oscillators. The distribution of the cyclic relative phase, which enables the detection of preferred phase differences irrespective of phase jumps, is defined as the modulus of the relative phase:

$$\psi_{n,m} = \omega_{n,m} \bmod 1, \tag{2.4}$$

SI can then be calculated from the distribution of the cyclic phase difference either based on Shannon's entropy or conditional probability. As can be seen from the definition in Eq. (2.3), SI can be used to estimate phase coupling both within one frequency and between different frequencies. Other measures have also been derived for quantifying cross-frequency coupling between neuronal firing rates and the phase of an oscillatory component, between amplitudes of two signals, or between the amplitude of one and the phase of the other signal (Bragin et al., 1995; Schack et al., 2002; Canolty et al., 2006). When studying oscillatory coupling, it is important to note that activity at different frequency bands may have distinct synchronization properties, especially regarding their spatial extent. For example, it was shown that beta-band

oscillations can synchronize over long conduction delays, where as gamma-band oscillations cannot (Kopell et al., 2000). This finding supports the view that gamma rhythm may be responsible for local computation, whereas beta-band activity may support interactions between more distant cortical areas (von Stein et al., 1999).

Cortical areas may also interact through information flowing dominantly from one cortical site to the other. Various measures for estimating this type of coupling between electrophysiological time-series have been proposed, such as Granger causality (Granger, 1980), Directionality Index (DI; Rosenblum and Pikovsky, 2001), Partial Directed Coherence (PDC; Sameshima and Baccala, 1999) and Directed Transfer Function (DTF; Kaminski et al., 2001). These methods can roughly be divided into two categories. The first category (Granger causality, PDC, DTF) uses autoregressive models to estimate predictability of time-series based on information contained in other time-series. Namely, they divide linear dependence between two time-series (X,Y) into linear influence from X to Y, Y to X and their instantaneous influence (Geweke, 1982, 1984). Furthermore, both Granger causality and PDC can separate direct causal influence between two signals from influence mediated via other signals. The second category (Directionality index) estimates the transfer of information from the instantaneous phases of the signals. This is done by estimating whether for one oscillator the phase difference between two time-points depends on the phase difference of the other oscillator, and vice versa. The estimation is based on fitting the dependency of the phase increment on both signals' phases, and by using this fit to calculate the cross-dependencies of phase dynamics of the signals.

2.3.2 Evidence from intracranial recordings

The first findings of population-level interactions between cortical areas came from intracranial recordings in cat visual cortex (Gray et al., 1989; Engel et al., 1991). Separate areas in the visual cortex were found to interact, and, importantly, their interaction was influenced by the properties of the visual stimuli. Later, it was discovered that synchronized firing was not limited to activity relating to stimulus processing but could occur during action as well. Coherent oscillations were detected between nearby sensory and motor areas in rhesus monkeys performing a hand movement task (Murthy and Fetz, 1992). Data recorded in cats during coordinated movement tasks revealed that interareal synchronization occurred even between more distant areas, namely between visual and parietal areas and parietal and motor areas (Roelfsema et al., 1997). Correlated activity across brain regions thus seemed to have an important role in sensory-motor integration and memory (König and Engel, 1995). In the studies above, coherence or firing rate correlations were used in investigating cortical interactions. Both approaches are, at least on the macroscopic scale, dependent on the overall level of activity. Amplitude-independent PLS applied to intracranial recording in an epileptic patient performing a visual discrimination task showed that neurons in the hippocampus and frontal gyrus were phase-locked in the gamma band (Lachaux et al., 1999). Phase synchronization was also demonstrated for two epileptic patients in a visual short-term memory task (Tallon-Baudry et al., 2001), where separate

extrastriate visual areas became synchronized at 15-25 Hz during rehearsal of line drawings.

It has also been proposed that interaction between two cortical areas may occur at multiple frequencies (Friston, 1997). Evidence of cross-frequency coupling has been found in intracranial animal studies at the level of single neurons and local field potentials (LFP). For example, multiple studies have shown that theta rhythm in one area can modulate the firing rate, spike timing and the gamma power in another area (Bragin et al., 1995; Chrobak and Buzsaki, 1998; Buzsaki et al., 2003). In human studies, multichannel subdural electrocorticogram (ECoG) recorded over the left frontotemporal areas indicated that the phase of theta rhythm modulated power in the high gamma band across a variety of behavioral tasks (Canolty et al., 2006). Moreover, the topography of the coupling was task dependent, suggesting that cross-frequency coupling may be a mechanism through which cortical areas integrate information in order to achieve adaptive behavior.

Coherence, phase-synchronization and cross-frequency coupling measure the undirected instantaneous influence between oscillators. Analysis of causal interactions has revealed, e.g., that that there are both bidirectional and unidirectional interactions in macaque visual cortex area TE, yielding direct evidence that it is possible for an area to feed information to another both in reciprocal and nonreciprocal fashion (Freiwald et al., 1999).

2.3.3 Evidence from EEG/MEG: sensor level

In most of the human electrophysiological studies that have aimed at elucidating cortico-cortical connectivity, the analyses have been done on EEG and MEG sensor level (Classen et al., 1998; Gerloff et al., 1998; Sarnthein et al., 1998; Andres et al., 1999; Miltner et al., 1999; Rodriguez et al., 1999; von Stein et al., 1999; Weiss and Rappelsberger, 2000; von Stein et al., 2000; Simões et al., 2003). Stronger interactions in multiple frequency bands (alpha, beta, gamma) have been reported during, e.g., motor, visuomotor, working memory and learning tasks (Classen et al., 1998; Gerloff et al., 1998; Sarnthein et al., 1998; Andres et al., 1999; Miltner et al., 1999). Coherence between areas may also decrease during certain tasks. For example, coherence between visual and motor areas was studied in a visuomotor tracking task, a motor task, a visual task and a motor task in the presence of a visual distractor, compared to rest (Classen et al., 1998). The visuomotor task resulted in increased coherence between EEG electrodes over the visual and motor cortex, whereas coherence was decreased when the subjects performed the motor task while a distractor was present. The motor task and the visual task alone did not result in changes of coherence, suggesting that coherence directly measures cooperativity between cortical regions. If this is the case in general, coherence analysis could be used in evaluating participation of regions during a task (in a cooperative manner), even when the overall level of activation in the areas would not exceed detection threshold.

EEG recordings have also shown that certain areas, as represented by electrodes placed over them, can elicit both increased activation and increased coherence, and not necessarily at the same frequencies. For example, during internally and externally paced

finger movements, both power (at 9-11 Hz) and coherence (at 20-22 Hz) increased over the contralateral sensorimotor areas (Gerloff et al., 1998). Furthermore, the internally paced condition resulted in larger increase of coherence, and also in an additional pre-movement activation, suggesting that internal pacing sets stronger demands on the motor system than external pacing. Motor control may thus be based on an oscillatory network which is modulated at least at two levels, i.e. oscillatory power and inter-regional coupling. If this pattern applies also to other cortical systems, their accurate characterization requires that one must be able to quantify both the levels of activation and interactions and test, for each case, whether they are modulated independently or in concert.

Similarly to intracranial recordings, amplitude independent measures have been used at the sensor level in quantifying cortico-cortical interactions. Analysis of sensor level recordings from a Parkinsonian patient revealed that the electromyogram (EMG) recorded from the moving arm muscle was synchronized with MEG sensor signals, and also that signals recorded over the motor cortex and premotor cortex were synchronized during tremor (SI; Tass et al., 1998). PLS has also been applied to EEG and MEG sensor level recordings to quantify phase synchronization (Rodriguez et al., 1999; Simões et al., 2003). When subjects viewed ambiguous stimuli that could be perceived either as faces or as meaningless shapes, phase synchronization in the gamma band across cortical sites depended on the percept while the stimulus itself was the same (Rodriguez et al., 1999). This finding indicated that internal synchronization, independent of the stimulus-induced activation, is a crucial element in generating a cognitive percept.

Cross-frequency coupling, in turn, has been detected in many intracranial recordings on animals and occasionally in humans (Mormann et al., 2005; Canolty et al., 2006), but reports at the EEG/MEG sensor level are scarce. When human subjects performed mental arithmetics, cross-frequency coupling at MEG sensor level emerged (Palva et al., 2005). There were multiple types of cross-frequency couplings, and the task load specifically influenced phase coupling between alpha and gamma band. The results implied that cross-frequency coupling may be an important mechanism for integrating spectrally distributed processing, and that it may directly reflect cognitive demands.

2.3.4 Evidence from EEG/MEG: source level

Unfortunately, the spatial specificity of EEG/MEG sensor level information is rather limited and, therefore, making inferences of the specific cortical locations and distinguishing nearby regions from each other, based on sensor-level data alone, is difficult. Intracranial recordings in humans can be done only in the rare cases of patients with implanted depth electrodes or during surgery. This limits substantially the amount of studies that can be done, and also the variety of experimental conditions that can be studied. Thus, it is of utmost importance that cortico-cortical interactions can be imaged on the cortical level. Apart from the work included in this thesis, there have been only a few attempts to do so with EEG/MEG (Ioannides et al., 2000; David et al.,

2003; Cosmelli et al., 2004; Jerbi et al., 2007). The approaches used in those studies can be divided into two categories.

In the first category, regions of interest are first localized in the brain based on their high level of activity. In a visual identification task of objects and emotional facial expressions, regions of interest (ROI) were defined by collecting evoked responses and localizing their cortical generators with magnetic field tomography (MFT) (Ioannides et al., 2000). Analysis of interactions between these ROIs revealed that coupling between the right posterior calcarine sulcus and fusiform gyrus differed for dissimilar objects, and that coupling between the right fusiform gyrus and amygdaloid complex differed for dissimilar expressions. In a visual binocular rivalry study with faces and expanding rings, a frequency tagged signal was first used to localize areas that showed activation at the tag frequency (Cosmelli et al., 2004). The localized areas consisted of extrastriate visual cortex, temporal pole and parietal and frontal areas. Subsequent phase synchronization analysis showed that interaction between occipital and frontal regions was dynamically modulated by the perceptual dominance.

In the second category of studies, external reference signals were used to localize a cortical reference area, enabling subsequent mapping of cortico-cortical interactions. In a visuomotor tracking task, a cortical reference area was localized by evaluating coherence between the hand-movement speed and cortical signals (Jerbi et al., 2007). Cortico-cortical coherence was estimated by first evaluating time-courses of activity at all cortical locations, and then calculating coherence between those locations and the reference area. The results revealed that the visuomotor network consisted of both subcortical and cortical areas.

In recent years, the concept of causal information flow between areas has become a popular topic. Most studies have concentrated on improving the methodology and verifying the main concepts with simulated data (Sameshima and Baccala, 1999; Baccala and Sameshima, 2001; Chen et al., 2006; Astolfi et al., 2007). Some EEG studies have reported directed interactions in the brain by first estimating cortical activity in ROIs, and then applying either directed transfer function, partial directed coherence or structural equation modeling (SEM) to estimate the directed information flow between these regions (Astolfi et al., 2005a, 2005b, 2007). Attempts have also been made to use fMRI priors to constrain the EEG source localization before quantifying connectivity between areas (Babiloni et al., 2005). The analysis of real data in these studies has been restricted to only a few subjects, instead of a thorough group analysis, thus limiting the possibility of making inferences on the nature of dynamical interactions generally encountered in the human cortex.

In addition, connectivity and transmission times between cortical areas can be investigated by combining high-resolution EEG with Transcranial Magnetic Stimulation (TMS) (Ilmoniemi et al., 1997). By localizing TMS-evoked electric responses in the brain it is possible to identify the spread of activation from the stimulated cortical site to other areas. This type of analysis has been applied, e.g., to investigations of sensorimotor and visual systems (Ilmoniemi et al., 1997; Komssi et al., 2002), and to determining how sleep affects cortical connectivity (Massimini et al., 2005).

2.3.5 Testing for significance of neural coupling

Regardless of the methods used to record electric neural activity and quantify the interactions, analysis of neural coupling can yield spurious results. First, two neural populations may seem to interact with each other when, in fact, the apparent coupling results from a highly consistent response to each stimulus. For example, two oscillating neural populations could be observed to be phase-coupled with each other if both their phases always lock to the stimulus without any noticeable jitter. In this case, surrogate data generated by mixing the trial order of one of the oscillators could be used to test whether the detected coupling resulted from the phases of the oscillators locking to each other or simply from highly reproducible locking to the stimulus (Lachaux et al., 1999). If the surrogate data yields similar phase-locking estimates as the original data, it indicates that the detected coupling did not result from specific interactions between the oscillators. In general, appropriate surrogate data should enable the significance of neural coupling to be evaluated, at least when the analyzed signals represent activation of distinct neural populations (Halliday et al., 1995; Palus and Hoyer, 1998).

However, apparent coupling between two neural sources may also be detected when activity from the same area is picked up at different sites. In EEG, this type of artifactual coupling can occur due to volume conductance that can cause activity originating in one location to be detected by a large number of electrodes. In MEG, a similar type of spurious coupling can arise since several sensors detect the magnetic field generated by electric current at one location in the brain. Estimating the activity at the source level does not remove the problem, as the same activity may erroneously be projected to different cortical locations. Both in sensor-level and in source-level analysis, surrogate data can be used to test for the significance of the coupling. In these cases, the surrogate data are designed to test specifically for coupling resulting from identical behavior of the two time-series. If the surrogate data were to indicate that the original coupling resulted from the two time-series having identical properties, it would be unlikely that the coupling represents real interaction between two independent neural populations. However, selection of an optimal surrogate data set can be problematic as the surrogate data must be designed to test for a specific effect and be justified by the data (Schreiber and Schmitz, 2000). Furthermore, for any one data set, surrogate data may be needed to test whether the signals at two locations represent the activity of the same source and whether the interaction between the signals reflects more than common stimulus locking.

2.4 Hemodynamic measures

For about 30 years it has been possible to image the hemodynamic changes that occur in the brain during task performance or stimulus processing using positron emission tomography (PET) (Ter-Pogossian et al., 1975). The main drawback of PET is that it requires delivery of radioactive tracers to the body. A less invasive way was developed as a modification of magnetic resonance imaging (MRI) that allowed imaging of the regional blood flow volume (Belliveau et al., 1991). The ensuing technique, functional magnetic resonance imaging (fMRI), has become the most widely used neuroimaging

technique. The greatest strength of fMRI lies in its millimeter scale spatial resolution. However, both hemodynamic methods also suffer from two limitations. First, their temporal resolution is, at best, on the scale of a hundred milliseconds. Second, these techniques give indirect information about the underlying neural processes. Both fMRI and PET have been used extensively in activation studies ranging from primary sensory processing to complex cognitive tasks.

2.4.1 Relationship between electromagnetic and fMRI signals

The results obtained with hemodynamic imaging techniques have both agreed and disagreed with the results from neurophysiological measurements. The differences have been explained, or sought to be explained, for example by neurophysiological processes being too transient to elicit a detectable metabolic/vascular effect. On the other hand, non-synchronous activity within neuronal populations could be undetectable with neurophysiological imaging techniques but still manifest in the hemodynamic response. Nevertheless, the exact relationship between neuronal and hemodynamic responses and, consequently, the manner in which hemodynamic measures yield information about the underlying neural processes remains unclear. To address these issues, the relationship between the most commonly investigated fMRI signal (Blood Oxygen Level Dependent; BOLD; Ogawa et al., 1992) and electric activity has been studied extensively over the recent years. For example, when the BOLD signal and both single-, multi-unit and local field potential recordings from monkey visual cortex were compared, the only electric signal that correlated significantly with the BOLD signal was the LFP, specifically in the gamma band (Logothetis et al., 2001). This finding suggested that the activation in that cortical area detected with BOLD contrast mechanism reflected input signals to and local processing in the area rather than its spiking activity. The stronger correlation between the BOLD signal and LFP compared with single- and multi-unit responses might also result from differences in spatial summation between the signals. Evidence supporting this view was obtained from recordings in the cat visual cortex (Kim et al., 2004). The correlation between the BOLD signal and single-unit responses at individual recording sites varied significantly, but over an area of several millimeters, averaged single-unit responses and BOLD signals were linearly correlated.

Correlation between electrophysiological and hemodynamic signals has also been investigated in humans, particularly for evoked responses and BOLD contrast (Menon et al., 1997; Grimm et al., 1998; Mulert et al., 2004; Whittingstall et al., 2007). These studies have often reported corresponding sources between the modalities, especially within primary sensory cortices. However, even for these primary sensory responses, the relationship between specific electric and hemodynamic components remains unclear. In a visual checkerboard stimulation task, the source generating the evoked response at 75 ms coincided with a positive BOLD activation, and the source generating the evoked response at 100 ms coincided with a negative BOLD signal (Whittingstall et al., 2007). This finding suggests the different electric responses may correlate with different parts of the delayed hemodynamic response and that it is

important to consider both the negative and positive BOLD activation in investigations of inter-modal correlations.

The correspondence between electrophysiological and hemodynamic imaging techniques has also been investigated with BOLD contrast and the band-specific electroencephalogram (Laufs et al., 2003; Mizuhara et al., 2004; de Munck et al., 2007; Oishi et al., 2007). A negative correlation between the alpha-band activity and BOLD was discovered in the parietal and frontal regions during relaxed wakefulness (Laufs et al., 2003). In this study, however, it was discovered that short-term fluctuations in the alpha-band activity were not reflected in the BOLD signal, but that fluctuation over tens of seconds explained the observed negative correlation with the BOLD signal. Thus, it may be that the alpha-band activity and BOLD signal are not necessarily directly linked, and that the detected negative correlation may reflect a more global correlation between the electrophysiological and hemodynamic signals. Furthermore, it should be noted that here, as well as in other studies comparing the hemodynamic and band-specific neurophysiological responses, the EEG sensor-level data was used as the neurophysiological measure. Thus, this type of analysis does not necessarily accurately quantify correlations between BOLD and neuronal responses within a cortical area, but a correlation between the hemodynamic activity in a given area and some type of mixed measure of electric activity over the whole brain.

The relationship between cortico-cortical interactions as revealed by hemodynamic and neurophysiological imaging has so far been addressed very rarely. A modeling study tested whether an underlying connectivity in neuronal activity can be detected with convolved hemodynamic responses (Horwitz et al., 2005). Electric connectivity between regions manifested itself in the ensuing fMRI connectivity, although less clearly. When the anatomical connectivity between the regions was reduced, the functional connectivity also disappeared. This study gives partial validation that functional connectivity between neuronal populations may be reflected in hemodynamic measures as well. Corroborating evidence was discovered from recordings in anesthetized rats (Lu et al., 2007). Here, different levels of anesthesia had a similar effect on both the hemodynamic and low-frequency electric correlation between the left and right somatosensory cortices. However, as the exact relationship between hemodynamic and neurophysiological measures, both for activation and coupling, remain unclear, it is difficult to obtain valid priors from one modality which could be applied to the other.

2.4.2 Hemodynamic coupling

Unlike in electrophysiological studies, where the analysis of cortico-cortical interactions has been mostly data-driven, in hemodynamic studies such analysis has traditionally been done based on modeling (McIntosh and Gonzalez-Lima, 1991; Friston et al., 1993a; Friston et al., 1993b; McIntosh and Gonzalez-Lima, 1994; Friston et al., 2003). Furthermore, for hemodynamic connectivity analysis, a difference was made early on between functional and effective connectivity, i.e., between instantaneous and causal interactions (Friston et al., 1993a; Friston, 1994). Structural equation modeling (SEM), a widely used approach, defines a model consisting of areas

and connections, and the strengths of the connections are determined by fitting the model to recorded data (Friston, 1994; McIntosh and Gonzalez-Lima, 1994). Subsequently, more advanced models of characterizing connectivity between cortical areas have been developed. Dynamical causal modeling (DCM) adds the level of neuronal connectivity to the modeling of hemodynamic coupling (Friston et al., 2003). Specifically, in SEM the changes in connectivity are seen directly as changes in the covariance structure of the hemodynamics, whereas in DCM external inputs modulate connectivity at the neuronal level, which then affects hemodynamic coupling.

Hemodynamic connectivity has been investigated through modeling during, e.g., imagery and visual and attentional tasks (Büchel and Friston, 1997; Friston and Buchel, 2000; Mechelli et al., 2004; Penny et al., 2004). For example, SEM analysis suggested that attention increased connectivity between visual area V5 and posterior parietal cortex in a visual motion tracking task, and that the prefrontal cortex modulated the afferent connection from visual area V5 to posterior parietal cortex (Büchel and Friston, 1997). A more detailed analysis of the data further revealed that activity in the prefrontal cortex sufficed to explain the modulatory effects in the connectivity (Büchel and Friston, 1998). DCM analysis, in turn, indicated that during visual perception and imagery of faces, houses and chairs, the modulatory effects of forward and backward connections could be separated between tasks: category-specific activations in the extrastriate cortex were modulated by the forward connections from visual areas during perception and by backward connections from the prefrontal cortex during imagery (Mechelli et al., 2004).

An alternate line of analysis in lieu of detailed examination of interactions between a few ROIs has been to look at correlations among a large number of areas. This type of analysis has been applied widely to resting state data to investigate the hypothesis that there is a default baseline mode of brain function which is suspended during specific goal-directed behaviors (Raichle et al., 2001). Based on functional connectivity estimates from resting state data, it has been proposed that the brain is divided into separate networks, which include the resting state network and, e.g., an attentional network (Greicius et al., 2003). Here, the network division is based on the clustering of positively correlated brain areas into separate groups (Cordes et al., 2002; Greicius et al., 2003; Fox et al., 2005). Moreover, this type of correlation analysis has revealed differences in the connectivity patterns between control subjects and Alzheimer patients (Greicius et al., 2004). The network properties of the brain have also been quantified by estimating correlation between all voxels (Eguiluz et al., 2005). Here, estimates of both local interconnectivity and mean number of links required to connect all voxels define the properties of the cortical network (Eguiluz et al., 2005; Achard et al., 2006). Estimation of connectivity between all voxels in this manner yields perhaps more information on the anatomical properties of the cortex than direct functional coupling, but it could prove useful in developing diagnostic tools for neurological disorders based on functional neuroimaging.

In addition, methods have been introduced that quantify effective connectivity without need for pre-defined models of regions of interest and their mutual connections. For example, an fMRI implementation of Granger causality was applied to a visuomotor mapping task. The results revealed directed influence from the left lateral prefrontal cortex and premotor areas to the left posterior parietal cortex (Goebel et al.,

2003). Instead of testing specific hypotheses about neuronal interactions in the form of constructed model, this method detects the direction of influence directly from the information contained in the data (Roebroeck et al., 2005). Causality, in fact, appears to be a necessary component of the analysis of BOLD interactions. It was shown that by including the history of the signals in the interaction analysis the results become more significant compared to when only the instantaneous coupling is considered (Lahaye et al., 2003).

2.5 Anatomical connectivity

Although direct evidence of neural information processing and integration comes from intracranial electric measurements and functional neuroimaging, anatomical imaging can chart out the underlying structures required for connecting segregated cortical areas. With diffusion tensor imaging (DTI), it is possible to identify white-matter fiber tracts that lead from one brain area to another (Basser et al., 1994a1994b; Mori and Van Zijl, 2002). This type of analysis can be useful in discovering the routes through which information may be transferred between cortical areas, i.e., whether two areas connect directly or through or third area. Also, it may be possible to evaluate whether there are changes in the anatomical connections and in ways that information can be transferred in the brain in different neurological disorders. DTI analysis has shown that anatomical connections constrain the activation seen with fMRI (Toosy et al., 2004). In the visual cortex, the BOLD signal change was correlated with the fractional anisotropy detected with DTI, indicating that the responses in the visual cortex were limited to areas to which there were anatomical connections from the optic radiation apex. DTI has also been used, for example, to identify ventral and dorsal auditory-language streams and to show that, in agreement with functional studies of auditory language processing, such connections are stronger in the dominant hemisphere (Parker et al., 2005). It should be noted, however, that thin fiber tracts are difficult to identify, and that it is practically impossible to distinguish when multiple fibers either cross or separate after closing in using DTI.

In short, there are a multitude of techniques and methods available for investigating cortical processing and integration of information non-invasively in the human brain. Different activation types (neurophysiological activity, hemodynamic signals) as mechanisms through which to study localized cortical processing have all their advocates. The same holds for integration of information. Some researchers endorse strong hypotheses in testing for connectivity, whereas others believe that data should be allowed to tell how cortical areas are connected. In addition, there are multiple measures that can be used to quantify coupling between cortical areas. For electrophysiological signals, two main types of mechanisms in particular have been emphasized in recent years. First, cross-frequency coupling, and specifically phase-to-power interaction, have been proposed to be sensible mechanisms from a physiological perspective (Jensen and Colgin, 2007). Others have advocated phase synchronization

between the participating neuronal groups as the mechanism through which the reciprocal interactions take place (Varela et al., 2001).

In the work presented in this thesis, I will focus on one imaging modality and two aspects of information processing and integration. Specifically, I will concentrate on the imaging of oscillatory activity and interactions at the cortical level using MEG. At the time when this project was started, it was not possible to directly evaluate cortico-cortical coherence, but quantification of interactions was done at the sensor level or by first localizing regions of interest and then estimating their mutual interactions. Here, we have developed methods that can be used to image, at the cortical level, coherence and oscillatory power in continuous tasks, and oscillatory power in event-related tasks, and we have applied those methods to real data. In addition to coherence and oscillatory power, we have applied measures such as SI, DI and Granger causality to quantify interactions between the identified cortical areas.

3 Magnetoencephalography

The transfer of information in neurons manifests primarily as electric currents, which in turn elicit magnetic fields. These fields can be measured from outside of the subject's head with magnetoencephalography (MEG). MEG is a totally non-invasive technique which can record the measured signals at a millisecond temporal scale, providing at the cortical level a spatial discrimination of 2-3 mm under favorable conditions (Hämäläinen et al., 1993). In this chapter, I will describe the physiological basis of the currents which generate the measured magnetic fields and the requirements that have to be met in order for the signals to be detectable. In addition, I will discuss some of the open questions regarding different types of signals which can be detected with MEG and portray the basics of the measurement procedure.

3.1 Neural currents and the origin of neuromagnetic fields

Neurons are the specialized cells which form the vast network responsible for signal processing and transfer in the brain. The human cortex contains on the order of 10^{10} neurons (Williams and Herrup, 1988.). An individual neuron consists of a nucleus within a cell body and extensions called dendrites and axons. Dendrites carry signals to the neuron, whereas axons convey the signal to the next neuron. The connection between two cells is called a synapse, which contains the pre- and postsynaptic endings, and a cleft between them.

Within a neuron, signal transfer is based on the properties of its cell membrane. The membrane divides the cell into intra- and extracellular spaces which have different ion concentrations. The concentrations are maintained by molecules located in the membrane which pump specific ions either into or out of the cell. With regards to the electric properties of the membrane, the most important pump is the Na-K pump which transfers the Na^+ ions out and K^+ ions in. The different potentials of the extra- and the intracellular spaces form an opposing flow to the one caused by the diffusion arising from the concentration differences. Equilibrium is reached when these flows are equal, which, in the resting state of the cell, results in a voltage of about -70 mV across the cell membrane. This potential is fundamental in the signal transfer along the membrane of a neuron. When a signal arrives at a patch of the neuron membrane, that patch depolarizes, i.e., the potential decreases, which causes Na^+-sensitive channels to open, allowing Na^+ ions to flow into the cell. This, in turn, further decreases the voltage difference. The depolarization also causes the neighboring ion channels to open, and an action potential, a constant-amplitude traveling wave along the membrane, is created. The action potential lasts only a few milliseconds before the cell is repolarized.

The electric properties of action potentials are such that they effectively form a quadrupole, the magnetic field of which decreases as $1/r^3$ as a function of distance r. Thus, they are difficult to detect with MEG which measures the signal at a minimum distance of a few centimeters from the surface of the brain. A more easily detectable signal is generated by the postsynaptic potential. When an action potential reaches the

synapse, transmitter molecules are released into the synaptic cleft. When these transmitters reach the postsynaptic side, the potential in the vicinity of the membrane is altered through permeability changes for specific ions. The potential change elicits an electric field and a current along the interior of the postsynaptic cell. The synaptic currents are effectively dipolar, and the magnetic field generated by them thus decreases approximately as $1/r^2$ as a function of distance r. Furthermore, although individually the synaptic currents are weaker than action potentials, the fact that they last longer and can occur in parallelly oriented synapses approximately simultaneously enables the summation of their fields. This ensuing field is the signal which is typically detected with MEG. Furthermore, it has been shown that this magnetic field, both for individual neurons and neuronal populations, is generated in the pyramidal cells of the cortex (Okada et al., 1997). A detectable magnetic field of this type requires that postsynaptic potentials of thousands of cells are synchronized. It has been suggested that this type of synchronous firing could reflect activity of cortical neurons that are driven by thalamo-cortical fibers (Hari, 1991). This mechanism has been suggested mainly for evoked responses. The thalamo-cortical connections are likely to contribute to the generation of the macroscopic cortical rhythmic activity as well, specifically in the form of intrinsic oscillations of neurons in the cerebral cortex and in the thalamic nuclei (Llinás, 1988; Steriade and Llinás, 1988; Steriade et al., 1990).

However, the exact relationship between the macroscopic oscillations and evoked responses remains unclear. A modeling study yielded evidence that both structural mechanisms, i.e., changes in coupling between regions, and dynamic mechanisms, i.e., changes in neuronal input, can generate evoked and induced rhythmic responses (David et al., 2006). It has also been shown that accounting for changes in intrinsic connections (reflecting local adaptation) improves the models that are used to explain the generation of evoked responses (Kiebel et al., 2007), and that feed-forward connections affect the evoked responses throughout the peri-stimulus interval, whereas feed-back connections substantially influence the responses only after 200 ms (Garrido et al., 2007). Whether the situation is comparable for induced rhythmic responses has not yet been resolved. In addition, it has been proposed that evoked responses, or at least many of their features, may be generated by phase resetting of oscillatory activity (Makeig et al., 2002; Penny et al., 2002). However, evidence exists also for different mechanisms being responsible for evoked responses and ongoing oscillations. In a visual stimulation study, phase resetting of ongoing alpha oscillations did not account for evoked responses (Mazaheri and Jensen, 2006). Instead, the evoked responses coincided with transient increases in stimulus-locked gamma oscillations. Furthermore, pain-induced suppression of oscillatory activity at both 8-13 and 15-25 Hz ranges was found to be negatively correlated with the corresponding evoked responses (Ploner et al., 2006). Thus, it is important to note that although synchronous post-synaptic potentials generate the detected magnetic fields both for evoked responses and rhythmic activity, it is as yet unclear whether the same dynamic and structural mechanisms give rise to these processes in neural populations.

3.2 Measurement of neuromagnetic fields

Even when thousands of neurons are active synchronously, the magnetic fields generated by electric activity in the brain are several orders of magnitude smaller than typical magnetic noise. In addition to fluctuations in the Earth's magnetic field, multiple environmental phenomena such as power lines, electric motors and vehicles cause transient noise which is much stronger than the signals originating from the brain. However, it is still possible to measure the cortically generated signal using Superconducting Quantum Interference Devices (SQUID) (Zimmerman and Silver, 1966), which are superconducting loops interrupted by one or two Josephson junctions. When a suitable bias current is applied, the magnetic field passing through the SQUID causes a periodically varying voltage. This voltage can be kept linearly proportional to the magnetic field by maintaining the SQUID at a constant magnetic field through a feedback current. Changes in the magnetic field can be measured by recording the amount of applied feedback current. In practice, the measurements must be performed in a magnetically shielded room to reduce the level of external noise. Superconductivity is currently feasible only at ultra-low temperatures, so the SQUIDs must be placed within an insulated container (called dewar), instead of being set directly on the subject's head. The subject is then placed on a chair or a bed underneath the dewar so that his/her head is as close to the SQUIDs as possible. The required insulation increases the distance to the subject's head by a couple of centimeters.

The devices used in MEG measurement are called neuromagnetometers. The sensors are laid in a grid formation that covers the entire scalp. The whole-head neuromagnetometers can sample the cortical signals without spatial aliasing (Ahonen et al., 1993). The neuromagnetometers used in this thesis work, Neuromag-122 (Fig 3.1) and Vectorview (Elekta-Neuromag^{TM}), have 122 and 306 sensors, respectively.

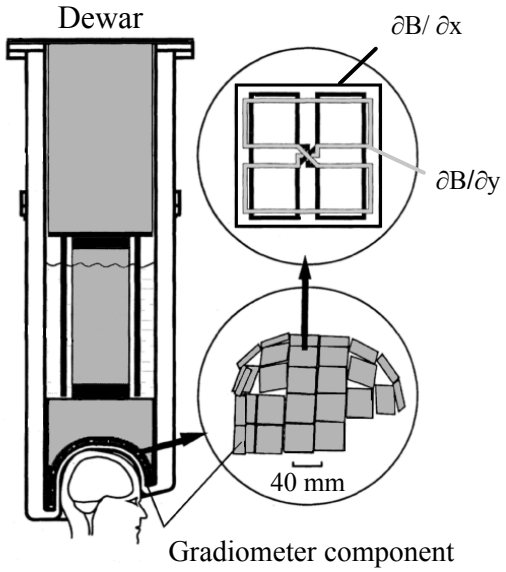

Figure 3.1: Neuromag-122 neuromagnetometer. Each sensor site contains two planar gradiometers which measure the change in magnetic field along orthogonal directions. Adapted from Hämäläinen et al. (1993).

In neuromagnetometers, the sensors typically consist of two parts, the SQUID and the flux transformer (divided further into the pick-up and signal coil). The magnetic field passing through the pick-up coil is coupled to the SQUID via the signal coil. The properties of the pick-up coil affect which kinds of signals are seen at the MEG sensor-level. A magnetometer (Fig. 3.2a), with the pick-up coil containing only a single loop, records the field component at a given location; gradiometers (Fig. 3.2b,c), which consist of both a pick-up coil and an oppositely wound compensation coil, measure the field difference between two locations (Hämäläinen et al., 1993). In axial gradiometers (Fig 3.2c) the pick-up and the compensation coils are set on top of each other, whereas in planar gradiometers (Fig 3.2b) the opposing loops are both set on the same plane. The main principle in gradiometers is that a homogeneous field causes opposing flux through the oppositely wound coils. Thus, gradiometers are insensitive to homogeneous magnetic fields which are likely to be caused by signal sources further away. Accordingly, gradiometers are more suitable than magnetometers for recording cortical activity when magnetic disturbances resulting from external noise sources are present. Furthermore, it has been shown that planar gradiometers record signals from a more restricted area than axial gradiometers (Hämäläinen et al., 1993). Thus, although for typical source localization different types of gradiometers are equally accurate, recordings in a noisy environment can benefit from the use planar gradiometers.

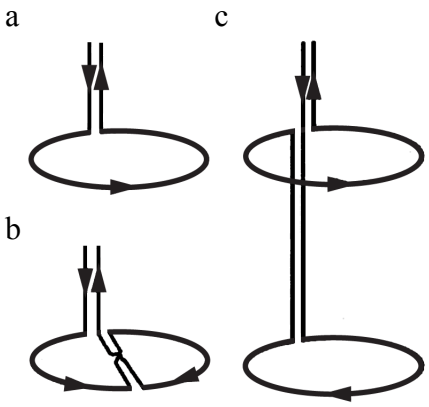

Figure 3.2: Three different types of flux transformers. a) A magnetometer contains a single loop, whereas b) a first-order planar gradiometer has a double-D structure and c) a first-order axial gradiometer is composed of oppositely wound serial pick-up and compensation coils. Adapted from Hämäläinen et al. (1993).

Both neuromagnetometer systems (Neuromag-122, Vectorview) that were used in the studies presented in this thesis contain two planar gradiometers at each recording site. The two gradiometers at each location are sensitive to field changes in orthogonal directions which increases the amount of information that can be obtained from the recordings. The Vectorview system also contains magnetometers in each of the 102 measurement sensor locations. In the analysis performed for this thesis, only data recorded by the planar gradiometers were used. The MEG analysis results are typically visualized by superimposing the identified sources on the subject's anatomical MR image. The co-registration between the modalities (MEG/MRI) is accomplished by

defining a common coordinate system using landmarks that are identifiable both in the MRI and on the head. Head position indicator coils, the locations of which can be determined both with respect to the landmarks and the MEG sensors, enable the alignment of MEG results to MRI space via the defined coordinate system.

3.3 MEG source modeling

The recorded MEG sensor signals yield information both on the timing and frequency content of cortical activation. However, as multiple source areas can contribute to the signal at each recording site, the sensor-level signals need to be decomposed into source-level electric activity in order to obtain an accurate spatiotemporal picture of neural activity. Although this determination cannot be performed unequivocally, reasonable constraints based on physiology and anatomy enable the solution of this neuromagnetic inverse problem. Here, the neural currents must be modeled, or else the solution constrained by some criterion, and the conductivity profile of the head needs to be defined.

3.3.1 MEG forward and inverse problems

The MEG forward problem consists of calculating the magnetic field generated by a known electric current. Typically the current is divided into two components; the primary current and the volume currents. Accordingly, the current density $\mathbf{J}(\mathbf{r}')$, i.e., the electric current at a given location, can be expressed as:

$$\mathbf{J}(\mathbf{r}') = \mathbf{J}^p(\mathbf{r}') - \sigma(\mathbf{r}')\nabla V(\mathbf{r}'), \tag{3.1}$$

where $\mathbf{J}^p(\mathbf{r}')$ is the primary current, $\sigma(\mathbf{r}')$ the macroscopic conductivity and $V(\mathbf{r}')$ the electric potential at location $\mathbf{r}'$. The primary current is concentrated in the vicinity of the cell, whereas the volume currents are distributed throughout the brain. Thus, localization of the primary current yields the neuronal activity of interest. If all the primary currents and the conductivity of the head are known, the magnetic field outside the head, based on the quasistatic approximation of Maxwell's equations and the Biot-Savart law (following derivations in Sarvas, 1987; Hämäläinen et al., 1993), can be calculated as:

$$\mathbf{B}(\mathbf{r}) = \frac{\mu_0}{4\pi}\left[\int_G \frac{\nabla' \times \mathbf{J}^p(\mathbf{r}')}{|\mathbf{r}-\mathbf{r}'|^3} dv' - \int_G \frac{\nabla'\sigma(\mathbf{r}') \times \nabla' V(\mathbf{r}')}{|\mathbf{r}-\mathbf{r}'|^3} dv'\right], \tag{3.2}$$

where μ_0 is the magnetic permeability in vacuum, $\mathbf{r}$ the measurement location and G denotes the conductor. Divergence of equation (3.1) yields:

$$\nabla \cdot \mathbf{J}(\mathbf{r}') = \nabla \cdot \mathbf{J}^p(\mathbf{r}') - \nabla \cdot \left(\sigma(\mathbf{r}')\nabla V(\mathbf{r}')\right). \tag{3.3}$$

From the quasistatic approximation of Maxwell's equations**,** since the divergence of a curl is zero, we see that $\nabla \cdot \mathbf{J}(\mathbf{r}')=0$. Accordingly, we obtain:

$$\nabla \cdot \mathbf{J}^p(\mathbf{r}') = \nabla \cdot \left(\sigma(\mathbf{r}')\nabla V(\mathbf{r}')\right). \tag{3.4}$$

This equation can be solved for V either analytically or numerically depending on the conductor medium. With a solution for V the magnetic field outside the head can be calculated according to equation (3.2). In a piecewise homogeneous conductor, $\nabla\sigma$ is non-zero only at boundaries, and the second term of equation (3.2) can be written as a sum of surface integrals over boundaries:

$$\mathbf{B}(\mathbf{r}) = \frac{\mu_0}{4\pi}\int_G \frac{\nabla' \times \mathbf{J}^p(\mathbf{r}')}{|\mathbf{r}-\mathbf{r}'|^3} dv' - \frac{\mu_0}{4\pi}\sum_{i=1}^{m}\sigma_i \int_{G_i} \frac{\nabla' V \times |\mathbf{r}-\mathbf{r}'|}{|\mathbf{r}-\mathbf{r}'|^3} dv', \tag{3.5}$$

where G_i denotes the regions with different conductivities σ_i.

In MEG analysis, the head is typically modeled as a spherically symmetric conductor. It is often a good approximation, as the results obtained differ only a little from those obtained with more accurate models (Hari and Ilmoniemi, 1986; Tarkiainen et al., 2003). Furthermore, it can be shown that in a spherically symmetric conductor, radial currents do not generate magnetic fields outside the conductor (Hämäläinen et al., 1993). As the head is approximately spherical, radial currents generate only a weak magnetic field outside the head, and MEG is most sensitive to tangential sources. In addition, in a spherically symmetric conductor, volume currents do not affect the radial component of the magnetic field outside the head (Hämäläinen et al., 1993). Although the sensors of an MEG system are typically positioned so that they mostly measure the radial field component, other field components are also recorded, and the generated tangential field components need to be calculated in the forward solution. In a spherically symmetric conductor model, the tangential field components can be computed without knowing the conductivity profile. However, if multiple layers are used in the conductor model, there are possible problems with numerical instability of the solutions, both for spherically symmetric and for realistically shaped conductors. In a multilayer spherically symmetric conductor, an isolated problem approach has been shown to yield accurate results (Hämäläinen and Sarvas, 1989). In addition, the currents on the skull and scalp were shown to contribute negligibly to the recorded field. Thus, for realistically shaped conductor models, one may avoid numerical problems and still obtain accurate results by using a single-layer brain-shaped homogeneous conductor model.

The neuromagnetic inverse problem refers to the estimation of the cortical currents that generated the measured magnetic fields. It is not possible to unequivocally determine the current distribution inside a conductor from knowledge of the electromagnetic field outside the conductor (Helmholz, 1853). This situation results from the fact that multiple source distributions can cause identical electromagnetic fields outside the conductor. Thus, it is mathematically impossible to identify the correct one among them. In practice, source models which are based on the physiology

of the brain can be used to circumvent this problem, enabling the estimation of the current distribution underlying the recorded magnetic fields.

3.3.2 Equivalent current dipole (ECD)

The most commonly used source model representing cortical activity is the dipole model (Kaufman et al., 1981; Tuomisto et al., 1983). In this framework, the primary current is modeled as a point-like current dipole. The dipole is a good approximation of coherent activation of a large number of pyramidal cells, observed some distance away from the active cortical area (Baillet et al., 2001). The model consists of a dipole with an orientation and strength, defined at a specific location:

$$\mathbf{J}^p(\mathbf{r}) = \mathbf{Q}\delta(\mathbf{r} - \mathbf{r}_q)\,. \qquad (3.6)$$

Here $\mathbf{Q}$ is the current dipole, $\mathbf{r}_q$ its location and $\delta(\mathbf{r})$ is the Dirac delta function. The location and the orientation of the dipole can be determined by finding the best fit to the data using a nonlinear least-squares search (Tuomisto et al., 1983). This search is typically done at a single time-point, and temporal correlations are ignored. It is also possible to construct a multi-dipole model by identifying active source areas separately at different time points. If the sources overlap both spatially and temporally, a multi-dipole calculation that incorporates several dipolar sources, maintaining their positions, can yield correct results (Scherg et al., 1989). This procedure takes into account the spatiotemporal course of the signals as a whole, instead of individual time samples. Dipole modeling can be used for localizing oscillatory activity as well. The recorded MEG data are band-pass filtered and ECDs are estimated sequentially at regular time-intervals with least-squares fit to a chosen subset of sensors (Salmelin and Hämäläinen, 1995).

3.3.3 Minimum norm estimates

Alternatively, if one does not wish to assume activation of only a small patch of the cortex, distributed current configurations can be used to represent neural activity. The first approach of this type was called minimum norm estimate (MNE; Hämäläinen and Ilmoniemi, 1984). MNE transforms the recorded sensor-level data into brain-level current distributions, with the sole assumption that the activity is confined to a certain area or volume. In practice, a set of points inside a conductor is defined, representing all possible source locations. As the forward solution can be computed for known electric currents it is possible to obtain the fields generated by unit-strength sources at these locations. MNE seeks a combination of weights for these sources that both minimizes the norm of the current distribution and explains the recorded data. The assumption is that the source configuration with the overall smallest amplitude is the most likely to be correct. As the MEG sensors are located at a relatively long distance from the brain

(and as the recorded signals contain noise), the obtained source distributions are usually somewhat blurred (Uutela et al., 1999).

Minimum current estimation (MCE) is a subtype of minimum norm estimates (Uutela et al., 1999). In MNE, the minimized norm for the current is the L2-norm (absolute value squared), whereas in MCE the norm used is L1 (absolute value). The L1 norm results in more focal source estimates than L2 norm (Matsuura and Okabe, 1995), which might be neurophysiologically more feasible. A method for obtaining the minimum current estimates in the frequency domain (MCE_{FD}) has also been developed (Jensen and Vanni, 2002). In this method, the data are transformed into frequency space for each successive time segment. The source estimates are then obtained by calculating the minimum current estimates for every time segment at the frequency of interest and by averaging those estimates.

3.3.4 Beamforming

A group of localization methods have been developed based on the principles of spatial filtering, commonly known as beamforming (Van Veen and Buckley, 1988; Robinson and Vrba, 1997; Van Veen et al., 1997; Gross and Ioannides, 1999; Sekihara et al., 2001). In beamforming techniques, the sensor-level data is filtered spatially so that estimates of activity are obtained simultaneously at all locations in the brain. The filter parameters are obtained by solving a constrained minimization problem:

$$\min_{\mathbf{H}} tr\left[\mathbf{HCH}\right] \quad \text{with} \quad \mathbf{HL}(\mathbf{r}_0, \mathbf{q}_0) = 1, \tag{3.7}$$

where **C** is (usually) the covariance matrix, **L** the forward solution for all sensors at location $\mathbf{r}_0$ for source orientation $\mathbf{q}_0$, and **H** is the variable containing the filter parameters to be solved. Thus, parameters are sought that minimize the total variance of the data while constraining the gain from the region of interest to unit output. This problem is solved separately at each location, or each set grid point, in the brain. Thus, one actually obtains multiple spatial filters which each have their own "band-passes", i.e., each filters activity in a manner specific to the location in question. Equation (3.7) represents the adaptive beamformer minimization, in which the spatial filter parameters depend on the data. Alternatively, the spatial filter weights could be determined independently of the data, i.e., merely based on the location where the solution is sought. The solution of the minimization problem in Eq. (3.7) has been shown to be similar to the minimum norm solution when *a priori* information of uncorrelated sources is included in the minimum norm solution (Mosher et al., 2003; Hillebrand et al., 2005). Thus, although these two approaches have been derived from different viewpoints, they are in fact very closely related, and their main difference lies in the definition of the data covariance (Mosher et al., 2003). The main benefit in beamforming is that the techniques do not require *a priori* assumptions about the number of active sources. The main drawback is that if sources are perfectly correlated, the beamforming solution fails. One should note, however, that valid beamformer solutions can be obtained even with quite high correlations (up to about 0.7; Hillebrand et al., 2005). Furthermore, even nearly perfectly correlated sources can be localized by

performing the beamformer estimation for different sources with separate selections of channels, e.g., by focusing on one hemisphere at a time (Herdman et al., 2003). Beamforming techniques have been refined further by incorporating permutation testing and estimation of distributions from multiple conditions to test for the significance of the estimates, both at individual and group level (Vrba and Robinson, 2001; Singh et al., 2003). In addition, it has been proposed that higher order covariance matrices yield better results than the traditional covariance matrix (Huang et al., 2004). A dual-source beamformer, where the forward solution patterns are calculated for source pairs instead of single sources, can be used to improve the beamformer estimates when highly correlated sources are present (Brookes et al., 2007).

3.3.5 Other techniques

Multiple other source modeling techniques have also been used in solving the MEG inverse problem (Mosher et al., 1992; Baillet et al., 1999; Mosher and Leahy, 1999; Baillet et al., 2001; Gavit et al., 2001; David et al., 2002; Grasman et al., 2004; Jerbi et al., 2004). Many of those approaches have aimed at finding the equivalent current dipoles more automatically, without selections made by the researcher (Mosher et al., 1992; Mosher and Leahy, 1999; Gavit et al., 2001), while other techniques seek to improve the localization by combining MEG and EEG data (Baillet et al., 1999). It is worth noting that a current dipole may not always be the best model for neural activity. For example, multipoles may yield more accurate and sensitive results than dipolar models, at least when large cortical patches are active (Jerbi et al., 2004).

All in all, there are various techniques that can be used in MEG to proceed from the sensor level to source level. It cannot be said that one is superior to the others. Each technique has its own strengths, and choosing the most appropriate method depends on the type of data being analyzed. Specifically, there are differences in how valid each model type is in explaining the data. In this thesis, I have focused on the development and application of a technique belonging to the group of beamformers. Because of the close relationship between the various MEG source localization approaches, the results should, nonetheless, be relevant for MEG imaging in general.

4 Dynamic Imaging of Coherent Sources: Methods (P1, P3, P4, P7, P8)

There were originally two main ideas behind the design of Dynamic Imaging of Coherent Sources (DICS). First, DICS transfers beamforming into frequency domain, enabling the imaging of oscillatory power in continuous tasks at the cortical level. Second, DICS enables the estimation of interactions, specifically coherence, at the cortical level without *a priori* defined regions of interest. The more recent development of event-related DICS (erDICS) adds the possibility of determining event-related modulation of rhythmic activity at the cortical level.

4.1 Basics of DICS (P1)

Cortico-cortical and cortico-muscular interactions have traditionally been estimated at the MEG and EEG sensor level. In DICS, beamforming enables the estimation of these measures at the cortical level. DICS uses a cross-spectral density (CSD) matrix to represent the sensor-level data. The CSD matrix carries information about the oscillatory components and their mutual linear dependencies. In earlier beamforming techniques, the covariance matrix was used to represent the sensor-level data and therefore the coherence could not be computed, since the required information was lost during the averaging across trials required for estimating the covariance matrix. DICS can be applied, in principle, to both EEG and MEG data; here, we focus on MEG data.

In DICS, the CSD between two signals $\mathbf{x}(t)$ and $\mathbf{y}(t)$ (representing data recorded by two sensors) is calculated using Welch's method of spectral density estimation (Welch, 1967). First, the signals are transformed segment-wise into Fourier space. Typically, partially overlapping segments that are ca. 1 second long are used. The transformed signals $\mathbf{X}(f)$ and $\mathbf{Y}(f)$ are then used to calculate the CSD for each segment:

$$\mathbf{C}(f) = \mathbf{X}(f)\,\mathbf{Y}^{*}(f), \tag{4.1}$$

where $\mathbf{Y}^{*}$ denotes the complex conjugate. The CSD representing the data is calculated by averaging the CSDs across segments. The CSD matrix is obtained by performing this calculation between all sensor combinations, including the sensor with itself. In addition to the MEG data, e.g., EMG or electro-oculogram (EOG) data may be incorporated into the matrix. The resulting matrix contains on its diagonal elements the CSDs of the signals with themselves, i.e., the power spectral densities. The cross-spectral terms are located on the off-diagonal elements. Coherence can be calculated according to equation (2.1) by dividing the squared magnitude of the cross spectral term with the power spectra of the corresponding signals.

The sensor level representation is transformed to the cortical level through a linear transformation. This transformation acts as a spatial filter/beamformer so that both power and coherence can be estimated at any location in the brain. The

transformation **A** is formed so that it passes activity in location **r** with unit gain while suppressing the interference from all other sources. This notion can be formulated as a constrained minimization problem:

$$\min_A[\varepsilon\left(\|\mathbf{AM}\|^2\right)+\alpha\|\mathbf{A}\|^2] \quad \text{with} \quad \mathbf{AL}(\mathbf{r})=\mathbf{I}, \tag{4.2}$$

where **M** is the Fourier transformed data (recorded by all sensors), ε denotes the expectation value, and the columns of **L**(**r**) contain the solution of the forward problem (i.e., the field generated at each recording site by a known current) for two orthogonal tangential unit dipoles at location **r.** The beamformer minimization also contains regularization defined by the parameter α, where a larger parameter yields a spatially more extended representation of a source. As can be seen from equation (4.2), the solution for transformation **A** depends on the data, i.e., DICS is an adaptive beamformer where the correlation between sources is exploited in the minimization of output variance. The solution of equation (4.2) is obtained by minimizing the corresponding Lagrange function (with $\varepsilon[|\mathbf{AM}|^2]=\mathbf{AC}(f)\mathbf{A}^T$, where $\mathbf{C}(f)$ is the CSD matrix), and the solution becomes (Gross and Ioannides, 1999):

$$\mathbf{A}(\mathbf{r},f)=(\mathbf{L}^T(\mathbf{r})\mathbf{C}_\mathbf{r}(f)^{-1}\mathbf{L}(\mathbf{r}))^{-1}\mathbf{L}^T(\mathbf{r})\mathbf{C}_\mathbf{r}(f)^{-1}\ , \tag{4.3}$$

where $\mathbf{C_r}(f)=\mathbf{C}(f)+\alpha\mathbf{I}$, The cross-spectral estimates between the four tangential source combinations at two location $\mathbf{r}_1$ and $\mathbf{r}_2$ can then be obtained according to:

$$\mathbf{C_s}(\mathbf{r_1},\mathbf{r_2},f)=\mathbf{A}(\mathbf{r_1},f)\mathbf{C}(f)\mathbf{A}^{*T}(\mathbf{r_2},f). \tag{4.4}$$

When $\mathbf{r}_1$ equals $\mathbf{r}_2$, the solution represents the power spectral density. One should also note that the cross-spectral density is calculated for the orthogonal tangential sources spanning all the possible tangential source configurations. If the singular values of $\mathbf{C_s}(\mathbf{r_1},\mathbf{r_2},f)$ differ sufficiently, i.e., $\lambda_1>>\lambda_2$, the cross spectrum can be attributed to sources with fixed orientations. In this case, the cross spectra can be estimated along the dominant source direction according to:

$$c_s(\mathbf{r}_1,\mathbf{r}_2,f)=\lambda_1\{\mathbf{C}_s(\mathbf{r}_1,\mathbf{r}_2,f)\}, \tag{4.5}$$

where $\lambda_1\{\}$ denotes the larger singular value of the expression in the braces. If there is no clear difference between the singular values, the trace of the cross spectrum is used instead.

In practice, the analysis is performed by determining a three-dimensional grid, which covers the brain with suitable intervals (5-10 mm) between grid points, and by calculating power and coherence estimates at each location. The results are presented as noise-normalized parametric statistical maps (pSPM) and as coherence maps where the values range from 0 to 1. These maps are overlaid on the individual anatomical MRIs. Figure 4.1 shows the power estimate at 8-13 Hz obtained with DICS from data recorded during rest.

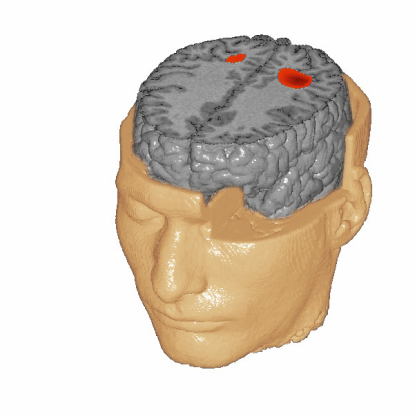

Figure 4.1: DICS pSPM at 8-13 Hz during rest.

In the mapping of cortico-cortical coherence, a cortical reference area needs to be identified first. This can be done, for example, by determining source areas that display high levels of oscillatory power at a given frequency. Figure 4.2a shows locations of four simulated sources and Figure 4.2b the pSPMs on the same axial slices. The two sources on the upper plane were coherent with each other, as were the two sources on the lower plane. Figure 4.2c shows the coherence maps when the leftmost sources on each plane were taken as cortical reference regions. The simulated data showed that both the localization and the DICS coherence estimates were accurate, also for highly correlated sources (coherence of 0.95) and regardless of the SNR.

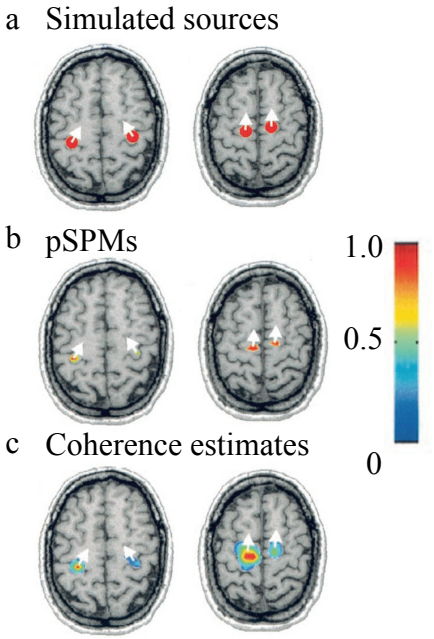

Figure 4.2: Simulated data. a) Locations of simulated sources, b) pSPMs and c) coherence estimates, with the leftmost sources on each plane selected as cortical reference areas. Adapted from P1.

4.2 MEG tomographic maps in the frequency domain (P3)

The properties of tomographic maps obtained with the frequency domain beamforming of DICS were then investigated in more detail. Two aspects were of primary interest: the spatial resolution of the estimates at different cortical locations and the confidence volumes of local maxima. The former measure yields information on the separability between neighboring source areas, the latter on the extent of the area where the true source is located with a given probability. These aspects were studied using both simulated and real data. We found that the spatial resolution varies with the cortical location, measured as the full width at half maximum (FWHM). Specifically, with uniform SNR at all locations in the brain, the resolution is worst in the deep areas, as is to be expected (Tarkiainen et al., 2003), but also in the more frontal areas where the sensor coverage is poor (Fig 4.3a). Thus, it may be difficult to separate sources of activity originating in frontal areas from each other, and coherence estimates can more easily yield spurious results within the frontal cortex than elsewhere in the brain. Coherence resulting from such leakage between spatial filters, i.e., due to the same signal detected at multiple sites (see leakage of spatial filters; Van Veen and Buckley, 1988), can be detected and rejected using surrogate data (Halliday et al., 1995; Palus and Hoyer, 1998; Faes et al., 2004), but the original localization with DICS might be misleading. However, for real recorded data, the SNR in different locations varies and this effect needs to be taken into account when the resolution of the tomographic maps are considered. The oscillatory power at each location can be used as an estimate of the SNR. Figure 4.3b portrays oscillatory power at 7-13 Hz for a 5-min recording when the subject was resting with eyes open. When this power map was used in estimating the FWHM, a clear reduction (i.e., improvement compared to the uniform SNR condition) was detected in the sensorimotor and occipital areas (Fig 4.3c), corresponding to the maxima of the power estimates.

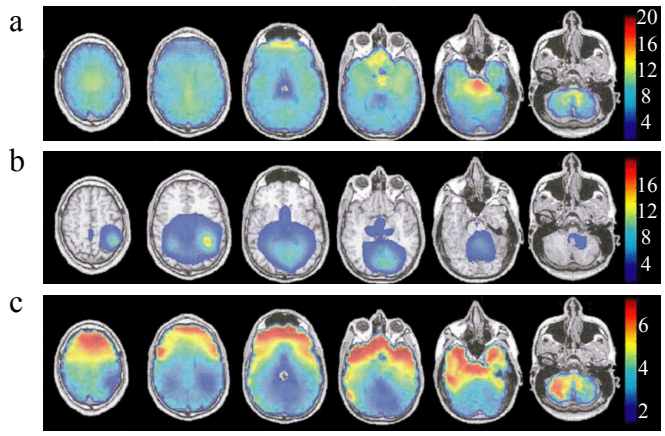

Figure 4.3: Resolution of DICS power estimates on six different axial slices. (a) The FWHM (in mm) at SNR 20 dB. (b) The ratio of power to noise at 7-13 Hz during rest. (c) The FWHM (in mm) at 7-13 Hz during rest. The oscillatory power at each voxel was used as an estimate of the SNR. Adapted from P3.

The confidence volume of the DICS localization was investigated using bootstrapping (Efron, 1979). The main benefit of bootstrapping is that it does not require assumptions about the distribution of the data. In practice, the calculation was done by using the segment-wise cross-spectral densities. A selected number of these segments were drawn randomly from the population, averaged and used to localize the maximum power. The random draw was repeated a large number of times to obtain a distribution and, subsequently, a confidence volume for the localization of the maximum. Here, this procedure was used to test the localization of the 7-13 Hz maximum for data recorded while the subject was resting with his eyes open. Figure 4.4 shows the probability map when 300 segments were used in the bootstrapping (300 seconds of data), and the bootstrapping was performed 10000 times. The small confidence volume demonstrates that the DICS localization is highly reliable, at least when there is enough data.

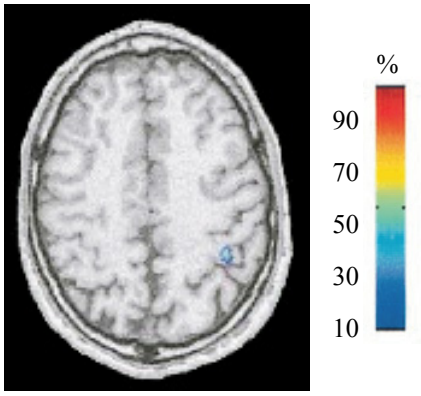

Figure 4.4: Probability map for localization of 7-13 Hz component during rest, obtained using bootstrapping. Adapted from P3.

It is also important to estimate how the length of the recording affects the confidence volume. We tested data segments of 30, 60, 120, 180 and 300 seconds. Table 4.1 summarizes the results. The confidence volume increased substantially for shorter data segments, but for segments longer than two minutes the volume remained quite stable. Naturally, the exact segment length at which this stabilization occurs depends on the recorded data and the strength of oscillations.

Length (s)	95% (mm)	99% (mm)
30	8.5	11.9
60	3.5	4.9
120	1.8	2.3
180	1.5	2.1
300	1.5	1.5

Table 4.1: Confidence volumes (95% and 99%) for 30- to 300-second data segments, obtained using the bootstrap method. Adapted from P3.

4.3 Localization of rhythmic activity in continuous tasks (P4)

Various approaches have been used in MEG to localize rhythmic activity at the cortical level during continuous tasks. We investigated how DICS compares to two of these, namely to band-specific ECD (Salmelin and Hämäläinen, 1995) and MCE_{FD} (Jensen and Vanni, 2002). Both MCE_{FD} and DICS yield simultaneous estimates of oscillatory activity at all cortical locations. In band-specific ECD, dipoles are fitted sequentially to data recorded by selected subsets of sensors. At each time point, the best-fitting dipole is accepted if the goodness-of-fit value (Kaukoranta et al., 1986) exceeds and the confidence volume remains below pre-defined threshold values. The ECD results were displayed as dipole density plots. A regular grid covering the entire brain was formed, and the number of dipoles within a set distance from each grid point was calculated. The resulting map showed the density of dipoles at each cortical location, which can be compared with the distributed maps of DICS and MCE_{FD}.

Based on analysis of both simulated and real recorded data, we found that all three methods gave fairly similar results. All methods were able to localize the principal sources of rhythmic activity quite well when the SNR was high. However, when the SNR was reduced, dipole modeling tended to fail. In addition, we tested how well the methods could separate neighboring source areas. When two simulated sources were placed in the brain at varying distances form each other, there were clear differences between the methods, as illustrated in Figure 4.5. When the two sources were 4 cm apart, all methods successfully found two active areas (Fig. 4.5c). When the distance between sources was 1 cm, all methods yielded one active area between the two real sources (Fig. 4.5a). However, at a distance of 2 cm between the sources, DICS was the only method that was able to separate the source areas from each other (Fig. 4.5b). Furthermore, when a more complex simulation of eight sources was used, DICS was the only method that was able to identify all sources.

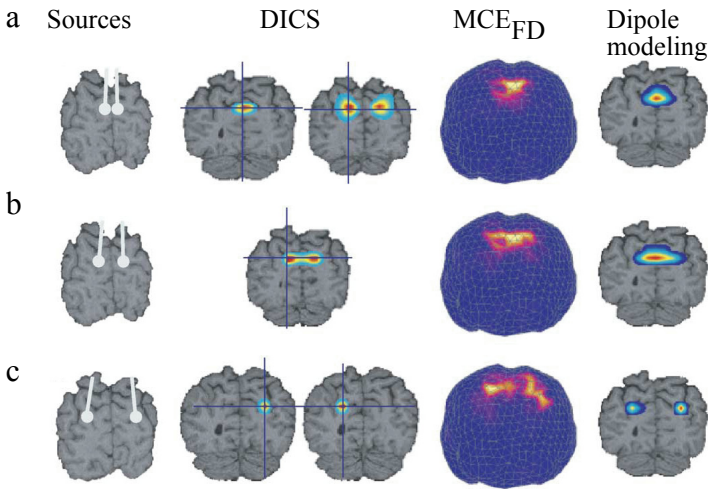

Figure 4.5: Separability of sources at distances of 1 cm, 2 cm and 4 cm with DICS, MCE_{FD} and band-specific ECD. a) All approaches yielded incorrect results at 1-cm distance, b) only DICS separated the sources at 2-cm distance, c) all approaches yielded correct results at 4-cm distance. Adapted from P4.

These types of clear differences were observed only on simulated data. On real recorded data all three methods yielded rather similar results. Figure 4.6 illustrates the localization of 10-Hz and 20-Hz rhythms in one subject when he was resting, eyes closed. In DICS, it is possible to incorporate the field generated by an identified source into the noise space. Thus, one may identify weaker sources whose activity is masked by a stronger source in the same frequency band. Using this approach, it was possible to identify source areas from real data which were not detected by ECD or MCE_{FD}. Similar signal space projection approaches could, in principle, be applied to MCE_{FD} and band-specific ECD as well. These types of approaches should be used with caution, however. If a source area is included into the noise space incorrectly (a mislocalized source), it may have an adverse effect on subsequent localization.

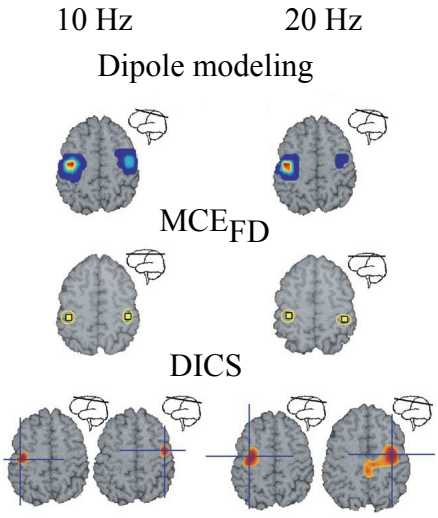

Figure 4.6: Localization of 10-Hz and 20-Hz components with dipole modeling, MCE_{FD} and DICS. The subject was resting, eyes closed. Adapted from P4.

4.4 Localization of event-related modulation of rhythmic activity (P8)

DICS was originally intended for analysis of rhythmic activity and coherence between cortical areas during continuous tasks. However, event-related modulations of rhythmic activity are also likely to be key mechanisms of information processing in the brain. The modified version of DICS, event-related DICS (erDICS), allows imaging of such modulations by using a filter bank based on Morlet wavelets that yield frequency distributions within short time intervals. The Morlet wavelet is defined as:

$$M(t, f_c, \sigma_t) = Se^{-t^2/2\sigma_t^2} e^{j2\pi f_c t} \tag{4.6}$$

where t is time, S a scaling parameter, f_c the center frequency of the wavelet and σ_t its standard deviation in the time domain. By replacing the Fourier transformation with wavelet decomposition in the calculation of the sensor-level cross-spectral density, one obtains a matrix containing both frequency and time information. Otherwise, the

erDICS beamformer is constructed analogously to DICS (equations 4.2 and 4.3), and the spatial filter solution becomes:

$$\mathbf{A}(\mathbf{r}, f, t) = (\mathbf{L}^T(\mathbf{r})\mathbf{C}_\mathbf{r}(f,t)^{-1}\mathbf{L}(\mathbf{r}))^{-1}\mathbf{L}^T(\mathbf{r})\mathbf{C}_\mathbf{r}(f,t)^{-1} , \qquad (4.7)$$

where $\mathbf{C}_\mathbf{r}(f,t)$ is the time-dependent cross-spectral density matrix. This modification allows calculation of time-dependent estimates of oscillatory power at frequencies of interest. Furthermore, by comparing different time instances (activation vs. baseline), it is possible to identify both increases and decreases of rhythmic activity in the brain.

We tested two approaches for applying the time-dependent CSD to obtain power estimates at the cortical level. In the first method, the time-dependent CSD matrix was averaged across trials, and the resulting mean CSD was used to beamform the recorded data to the cortical level. From these time courses, the oscillatory power was calculated by band-pass filtering the data and evaluating the instantaneous amplitudes via the Hilbert transform. In the second approach, the power maps were calculated separately for each trial using single-trial time-dependent CSDs. The final power estimate was obtained by averaging these individual power maps. Statistical significance of the estimates can be evaluated by permutation of time courses (first approach) or individual power maps (second approach).

These two approaches were compared using a simulation where three sources were set to oscillate at around 20 Hz. The activity of the sources was initially suppressed after an event, followed by a rebound. Figure 4.7a shows the results from the mean CSD and single-trial CSD approaches. The mean CSD approach yielded an accurate and focal representation of the correct source areas, whereas the single-trial CSD approach yielded an estimate that was more spread out both in time and space. For the mean CSD approach, the locations of the maxima of the erDICS maps were always at the correct location down to SNR of 1/15. For the single-trial CSDs, the maximum suppression was detected at an incorrect time-instance. The reason is that the temporal resolution of wavelets was too low to separate events close in time, an effect that is enhanced when the power maps are estimated at low SNR, which is avoidably the case for single trials. When the temporal separation between the suppression and the rebound was increased, the single-trial approach identified the suppression at the correct time, although the estimates were still spatially more extended (Fig. 4.7b).

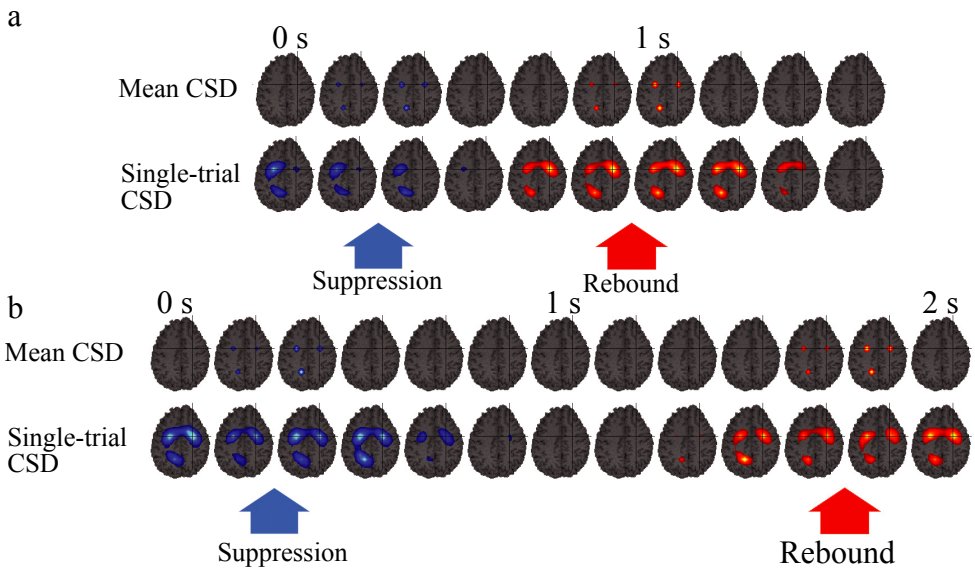

Figure 4.7: erDICS power maps for simulated data with mean CSD and single-trial CSD approaches, when the end of suppression and start of rebound were a) 300 ms and b) 1200 ms apart. Adapted from P8.

The statistical evaluation of the results was performed using maximum statistic permutation testing. The voxel-based random permutation test was implemented by first calculating a statistic (a common Student's t-test) for the two distributions (trial-to-trial power levels in the "active" and "baseline" intervals). The samples in the two distributions were then permuted randomly and a new t-value was calculated for this distribution. The test distribution of t-values was obtained by repeating this step 5000 times and by recording all the t-values. The p-values at each voxel were then estimated by comparing the original t-value to this distribution. Furthermore, the maximum and minimum t-values from the test distributions in each voxel were collected, defining new test distributions across voxels. The final p-values in each voxel were estimated by comparing the original t-values to the maximum/minimum distributions.

As the mean CSD approach yielded spatially more focal and temporally more accurate results for the power maps, we performed the statistical testing only for this approach. In the procedure we included a fourth source in the simulation. This source elicited a strong (artefactual) rebound in 1/20 of the trials. Thus, apparent power in this area did not result from systematic differences between time windows. Both the power and statistical estimates of the suppression yielded the correct results under reasonable SNR (Fig. 4.8a). The power estimates of the rebound showed a maximum at the location of the spurious source. However, the activity at this location did not pass the statistical testing (Fig. 4.8b).

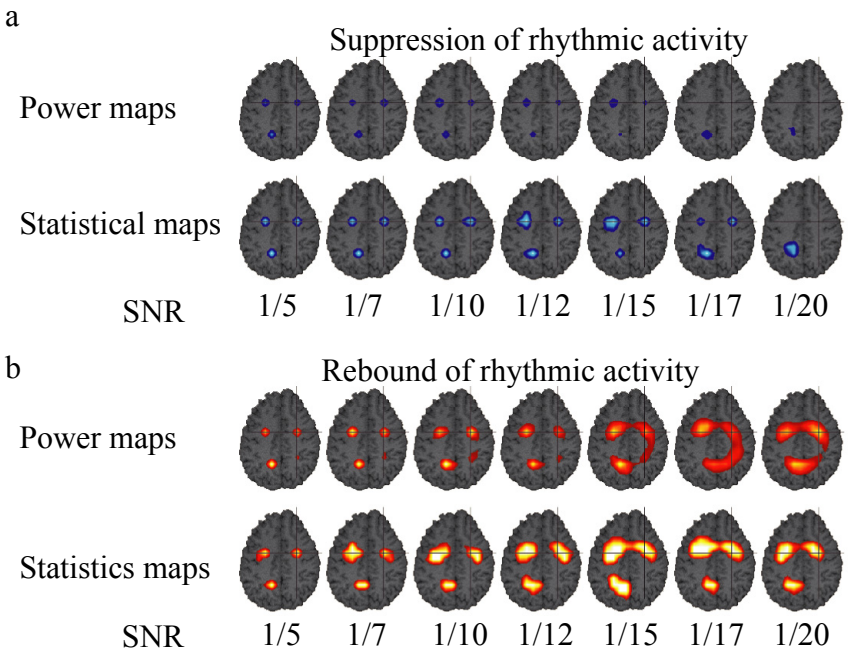

Figure 4.8: erDICS power and statistical estimates of a) suppression and b) rebound for simulated data at various SNR values. Adapted from P8.

We applied the method to two real datasets, one recorded during index finger movement and the other during silent reading of words. In the finger movement task, the sensor-level spectra showed strong reactivity at around 20 Hz. Both the power and statistical maps clearly showed contralateral activation of the motor cortex, as expected (Fig. 4.9a). In the silent reading task, the sensor-level spectra revealed modulation of activity at 7-14 Hz. The erDICS power and statistical maps showed salient involvement of four source areas (Fig. 4.9b). The identified areas accounted for 71% and 79% of the variance in the data for the right finger lift and for the reading data, respectively.

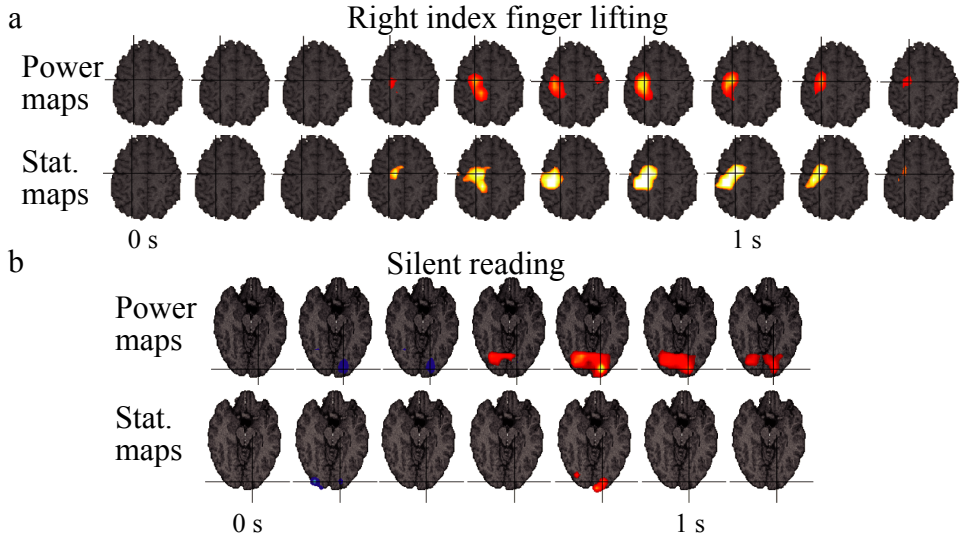

Figure 4.9: erDICS power and statistical estimates for a) right index finger lifting at 14-27 Hz and b) silent reading at 7-14 Hz. Adapted from P8.

4.5 Localization of interacting cortico-cortical networks (P1, P7)

In theory, interacting cortico-cortical networks could be identified by estimating coherence between all possible locations in the brain. This type of analysis, however, has multiple drawbacks. First, it is computationally taxing, at least when small voxel sizes are used. Second, it can be difficult to identify the relevant coupling from amongst a vast number of connections. In addition, there are specific problems when EEG/MEG data is analyzed in this manner. Specifically, in beamforming analysis, without constraining the coherence analysis to long-range coupling, leakage effects between spatial filters may easily dominate the obtained picture of connectivity. This is especially true if coherence analysis is also extended to deeper areas in the cortex. In addition, if there is no actual cortical activity around the voxel used as a reference in the mapping of cortico-cortical coherence, the obtained estimates can be quite misleading. Thus, in practice, it is better to first identify accurately a single cortical reference area, or a few areas, and then use them in localizing interacting cortico-cortical networks. This can be done by identifying cortical areas that show high levels of oscillatory activity or whose rhythmic activity is modulated by the task (Fig. 4.10a). Alternatively, coherence with external reference signals, such as EMG, may be used (Fig. 4.10b). It appears, however, that in many tasks oscillations in the relevant areas do not necessarily exceed the level of background activity. Furthermore, suitable external reference signals are often not available, especially in cognitive tasks. A more general approach is to calculate coherence between all voxel combinations, excluding neighboring voxels and brain areas in which the resolution of MEG is at its worst, and to identify voxels which show the highest number of connections to other regions (Fig 4.10c).

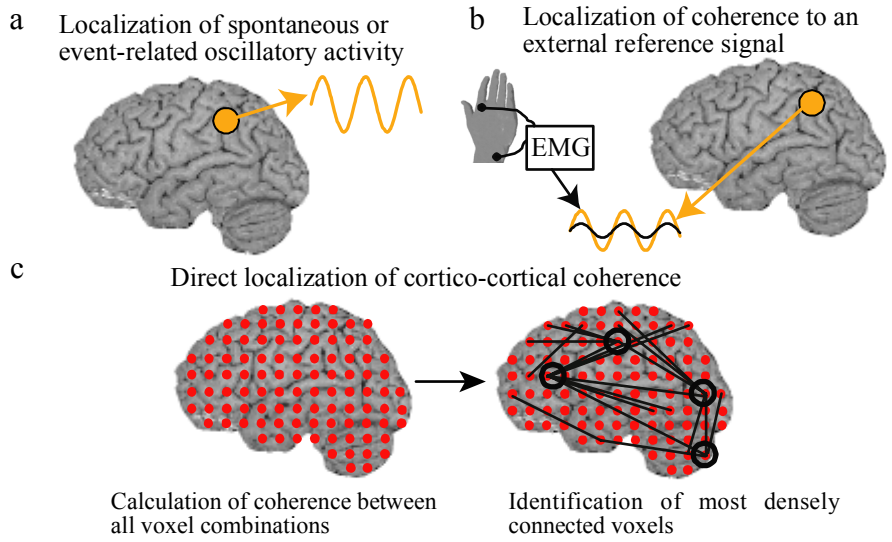

Figure 4.10. Identification of cortical reference areas based on a) oscillatory power, b) coherence with an external reference signal and c) direct estimation of cortico-cortical coherence.

4.5.1 Localization of interacting areas via oscillatory power and external reference signals (P1, P7)

In continuous tasks, the brain frequently shows spontaneous rhythmic activity that is present much of the time. This activity, and the areas that elicit it, may not necessarily be relevant to the performance of the studied task. Modulation of the spontaneous rhythms across conditions or their modulation in neurological disorders, however, may enable localization of more pertinent components of the network of interest. Figure 4.11 illustrates results from a Parkinsonian patient with right-sided tremor. Here, both pSPM (Fig. 4.11b) and coherence with EMG recorded from the arm muscles during the tremor (Fig 4.11a) pointed to the primary motor cortex (M1). Figure 4.11c depicts the cortico-cortical coherence where the left M1 served as the reference area and the other maximum corresponds to the premotor cortex. Although the interaction mapping in DICS is based on coherence, it is possible to evaluate other types of interactions for the identified ROIs. A spatial filter (Van Veen et al., 1997) was used to estimate time courses of activation at the defined locations. Figure 4.11d illustrates coherence and SI calculated between the estimated time courses at M1 and the premotor cortex. The synchronization between the areas was substantially increased as the Parkinsonian tremor started.

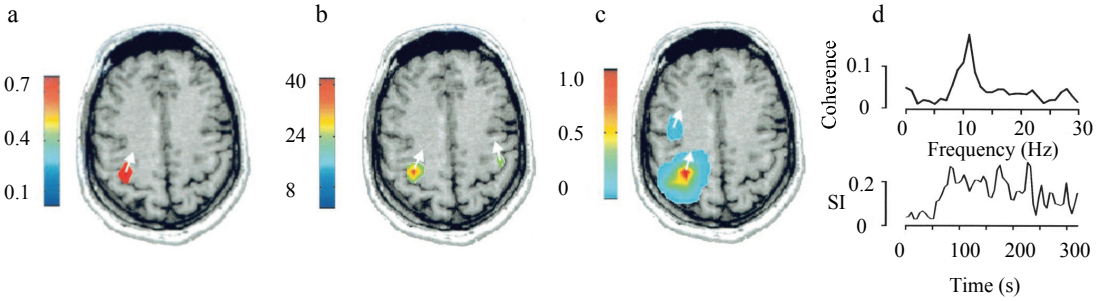

Figure 4.11: DICS estimates of cortico-muscular and cortico-cortical coherence during Parkinsonian tremor. a) Cortico-muscular coherence, b) pSPM, c) cortico-cortical coherence and d) coherence and synchronization index between M1 and the premotor cortex. Adapted from P1.

When a single, functionally comparable, cortical reference area can be identified across subjects, it enables robust investigation of cortico-cortical networks at the group level. Coherence can be calculated from this common reference area and the resulting maps can be subjected to group-level analysis. Figure 4.12a illustrates a set of simulated interacting areas, and 4.12b the group-level coherence map obtained with a one-sample t-test, using SPM2 software (Wellcome Department of Imaging Neuroscience, University College London, United Kingdom, http://www.fil.ion.ucl.ac.uk/spm/spm2.html). The common reference area was identified based on coherence with an external reference signal, and a one-sample t-test across subjects was calculated for the spatially normalized coherence maps that had been calculated starting from this area. The analysis revealed all coherent sources and two additional spurious areas that exceeded the threshold ($p<0.05$) of the one-sample t-test.

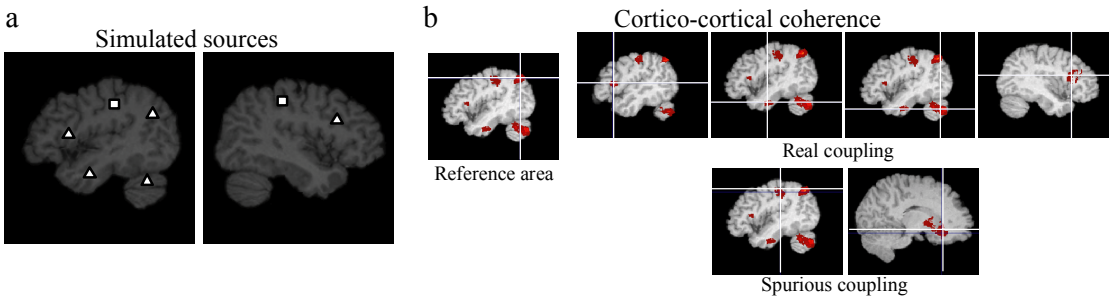

Figure 4.12. Group-level mapping of cortico-cortical coherence, starting from a common reference area that was identified based on coherence to an external reference signal. a) Locations of coherent sources (triangles) and noncoherent sources (rectangles) projected to one left- and one right-hemispheric slice. b) Cortico-cortical connections at the group level, starting from a common reference area. In each view, the crosshairs indicate the maximum on which the slice was centered. Adapted from P7.

4.5.2 Localization of interacting areas directly via cortico-cortical coherence (P7)

When suitable external reference signals are not available and oscillatory power fails to reveal the areas of interest, one possible solution is to directly estimate cortico-cortical coherence, without selecting a specific reference area beforehand. In connection density estimation (CDE), one approach of this type, we divide the brain into voxels and compute coherence for all voxel combinations, excluding connections between neighboring voxels. CDEs are obtained by counting, for each voxel, the number of connections for which coherence exceeds a chosen threshold. As this analysis is aimed at identifying cortical reference areas, rather than identifying the entire network, the search space can be restricted to more superficial areas, or even to limited regions of interest. Such limitations can be used to reduce spatial filter leakage effects, as the areas where the resolution is worst can be excluded from the analysis. A similar benefit can be obtained by increasing the minimum length of accepted connections. Figure 4.13a illustrates the results of CDE for the simulated network shown in Fig. 4.12a, where coherence was estimated between voxels located more than 5 cm from each other and within 15 mm of the surface of the cortex.

If CDE leads to identification of a common cortical reference area across subjects, that area can be used for group-level mapping of cortico-cortical coherence in the entire brain. However, if the areas identified based on CDE are too variable for this approach, coherence mapping must be performed in individual subjects with each of the localized CDE maxima as starting points. Figure 4.13b shows the identified connections starting from the eight CDE maxima in Fig. 4.13a.

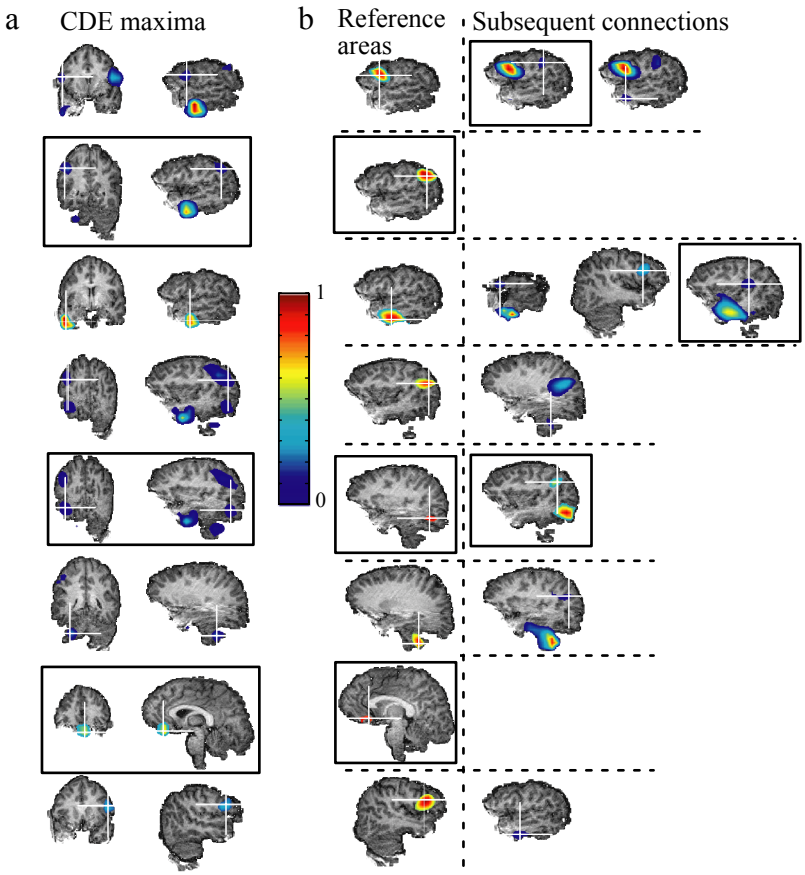

Figure 4.13. Network identification starting from connection density estimates (CDE). a) Focal maxima of CDE maps. Each point in these maps gives the number of connections from that voxel to all other voxels included in the search, normalized to the highest number of connections per voxel. b) Coherent connections (coherence > 0.1), starting from CDE-based reference areas. The left-most column portrays the coherence of a reference area with itself. Spurious reference areas and spurious connections are marked with a black box. Adapted from P7.

CDE can be performed either at individual or group level. The group-level analysis can be beneficial if its increased statistical power outweighs interindividual variability in node locations. Figure 4.14a illustrates the accuracy of CDE, performed at individual and group level, for three simulated datasets with different intersubject variability (9 simulated subjects; 0, 5-7 and 10-12 mm intersubject variability). The individual-level analysis resulted in localization of sources within, on average, 7 mm from the correct locus. The group-level localization was more accurate than the individual-level results only when there was no intersubject variability; otherwise the individual-level localization was more accurate. This indicates that in CDE the benefits obtained from increased statistical power of a larger subject population are relatively small. Accordingly, CDE should be used at the individual level whenever possible, as it is probably not realistic to assume that the intersubject variability of functionally corresponding areas would be less than 5 mm (Xiong et al., 2000).

The intersubject variability in the node locations also affects the localization accuracy of the final group-level network. The final network is identified based on consistency estimation of individual-level nodes, i.e., by calculating how many subjects have a significantly coherent nodal point within a specified distance of a voxel in normalized coordinates. Figure 4.14b depicts the accuracy of network identification, when either the node coordinate identified from the group map or the individually identified point closest to the group maximum was used to represent the node. When the intersubject variability was zero, the group-level localization was more accurate, and when the variability was large, individual-level identification was more accurate. However, at intersubject variability of 5-7 mm, there was no statistical difference between individual and group-level localization accuracies. Thus, in the final network identification, the increased statistical power obtained from group analysis was more useful than in CDE.

The specificity of CDE can be improved by limiting the coherence estimation to source areas in which current flow has an approximately constant orientation. This neurophysiologically reasonable assumption is based on the fact that MEG detects simultaneous activity in thousands of parallelly oriented dendrites in a small cortical patch. Thus, a source with a dominant direction of current flow is more likely to reflect accurate localization than a source with labile orientation. The orientation constraint is incorporated into DICS by evaluating whether the beamforming estimate at a given location can be attributed to a source with a fixed orientation. The main benefit of this constraint in CDE is that it reduces the effects of spatial filter leakage in identification of cortical reference areas. Specifically, CDE yielded fewer spurious areas and more of the real areas when coherence was estimated only between sources that had relatively fixed orientations (Fig. 4.14c).

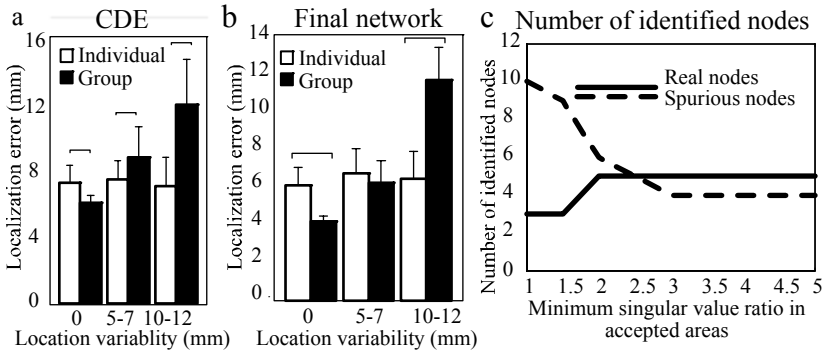

Figure 4.14: CDE accuracy, effects of orientation fixedness criterion, and accuracy of final network localization. a) Error in localizing the nodal points (mean + SEM) from individual vs. group-level CDE when the intersubject variability was either 0, 5-7 or 10-12 mm in three simulations. Significant differences (paired samples t-test $p<0.05$) are marked with brackets. b) Localization error in final network identification (mean + SEM) when nodal points were determined from group-level data and when nodal points were determined from individual results, for three levels of interindividual variability in node locations. c) Number of identified real (solid curve) and spurious (dashed curve) network nodes as a function of the singular value ratio (estimate of source orientation fixedness). Adapted from P7.

Real recorded data cannot be used to evaluate the accuracy of any method, but it is possible to compare different approaches and test to which precision they yield similar results. In a dataset recorded during slow finger movement, EMG-MEG coherence was successfully used to localize M1, enabling the mapping of cortico-cortical coherence and identification of the premotor cortex as a network node (Fig. 4.15a). The same two cortical nodes also emerged using CDE (Fig. 4.15b). The difference in localization of the two approaches was on average 8 mm, i.e., within the spatial resolution of MEG. Thus, although it is impossible to say which, if either, localization is correct in absolute terms, the results indicate that CDE can be applied in the localization of cortical reference areas also for real data.

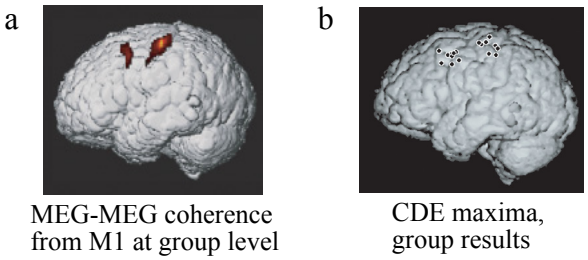

Figure 4.15: Identification of cortical networks at group level during slow finger movement. a) Localization of M1 with EMG-MEG coherence, and subsequent identification of premotor cortex with MEG-MEG coherence (group-level results). b) Identification of both the motor cortex and premotor cortex using CDE, in each of the nine subjects. Adapted from P7.

5 Dynamic Imaging of Coherent Sources: Applications (P2, P5, P6)

The developed methodology was applied to data collected in two separate experiments, one involving a motor and the other a reading task. The aim was both to localize coherent cortico-cortical networks participating in the performance of the tasks and to characterize the behavior of the networks in more detail using non-linear interaction measures. In addition, we compared the DICS localization results from the reading task to results obtained from earlier activation studies of language.

5.1 Localization of cortical interactions in a motor task (P2)

Continuous movements are perceived as smoothly changing, whereas in reality they exhibit pulsatile velocity changes at around 8 Hz (Vallbo and Wessberg, 1993). These changes have been thought to represent intermittent control from cortical motor areas. We sought evidence of such control by using DICS to characterize cortico-cortical interactions during slow finger movements.

5.1.1 Recordings

The data were collected from nine healthy, right-handed subjects while they performed continuous, self-paced horizontal flexion and extension movements with their right index finger. The recording was performed with Neuromag-122 MEG system, and the data were filtered to a band of 0.03–330 Hz and sampled at 1 kHz. EMG signals were recorded from the right first dorsal interosseus, flexor digitorum superficialis and extensor digitorum communis muscles.

5.1.2 Results

Movement discontinuities could be seen in all subjects both in the kinematic and EMG signals, and there was a salient peak in the EMG power spectra at 6-9 Hz. The EMG-MEG coherence estimation, using EMG from extensor digitorum communis muscle, revealed a significant coherence maximum in the left sensorimotor cortex in all subjects. The identified areas included both pre- and post-central parts, and the directionality index was subsequently used to separate the afferent and efferent components of the coherence maps. Figure 5.1 shows the group-level result from this analysis, with a clear separation between the primary somatosensory and motor cortex.

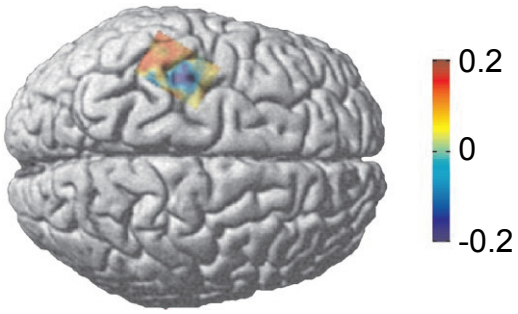

Figure 5.1: Direction of 6-9 Hz sensorimotor-muscle coupling. The DI between muscle and cortical activity was computed in the sensorimotor cortex for each individual subject. The individual directionality maps were spatially normalized and averaged across subjects. Blue and red colors represent predominantly efferent and afferent coupling, respectively. Adapted from P2.

M1 was taken as a cortical reference area, and coherence was calculated from M1 to all other brain regions. Group-level analysis of coherence revealed systematic interactions of M1 with the left premotor cortex, left thalamus and right cerebellum. SI and DI were used to further characterize the coupling between these regions. All areas were significantly phase coupled, and the dominant coupling directions led from cerebellum to thalamus, from thalamus to premotor cortex (PMC), from premotor cortex to M1, and from M1 to cerebellum (Fig 5.2). Apparently, synchronized rhythmic activity at 6-9 Hz in the cerebello-thalamo-cortical loop participates in transferring information in the control of slow finger movements.

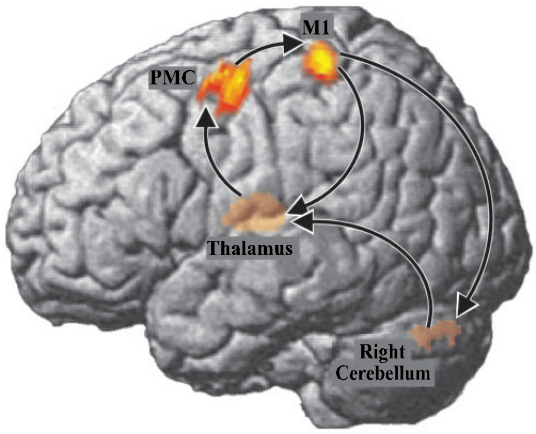

Figure 5.2: Control of intermittent finger movements. Spatial distribution of coherence, with the left primary motor cortex as the reference area. Only areas with $P<0.05$ (corrected, one-sample t-test) are shown. Arrows indicate the dominant coupling direction (mean DI). Adapted from P2.

5.2 Identification of connectivity in a reading task (P5)

In motor tasks, EMG-MEG coherence enables the localization of cortical areas that may serve as starting points in identification of cortico-cortical interactions. In cognitive tasks, suitable EMG or other external reference signals are not readily available. It is possible, however, to localize interacting cortical networks by directly identifying cortico-cortical interactions. We applied this type of analysis to a dataset recorded during continuous reading, and tested how the task difficulty affected coupling between identified cortical areas.

5.2.1 Recordings

The data were recorded from nine native English-speaking subjects during rapid serial visual presentation (RSVP) of words. In three 5-minute blocks, words forming a continuous story were presented at individually determined rates varying from 5 to 30 words per second. At the slowest rate, the entire story could be understood; at the medium rate parts of it, and at the fastest rate only individual words could be understood. In a fourth block, words were presented in a mixed order at the slowest rate, and in a control condition words and pseudo-words were presented at 3-second interstimulus intervals. The recording was done with a Vectorview MEG system, and the data were band-pass filtered at 0.03-200 Hz and sampled at 600 Hz.

5.2.2 Results

As there were no meaningful external reference signals available, CDE was used to identify cortical reference areas. Because the localized areas were too variable to identify a common reference area for all subjects, the cortico-cortical networks were determined separately for each subject. The CDE resulted in 7-11 reference areas and the subsequent estimation of coherence in the entire brain from these resulted in 12-18 candidate nodes per subject. Surrogate data were used to estimate the significance of coherence between these nodes, and areas passing the test were included in the final network for each individual subject. Figure 5.3 shows the maxima of the group level consistency test performed on these networks. This analysis revealed systematically coherent areas across subjects, specifically in the left hemisphere, including the inferior occipitotemporal cortex, medial temporal cortex, superior temporal cortex, anterior part of the inferior temporal cortex, precentral cortex, insula, prefrontal cortex, and orbitofrontal cortex. These areas have previously emerged in activation studies of language function or in experiments focusing on visual recognition and working memory (Nobre et al., 1994; Price et al., 1994; Ivry, 1996; Fiez and Petersen, 1998; Helenius et al., 1998; Petrides et al., 2002).

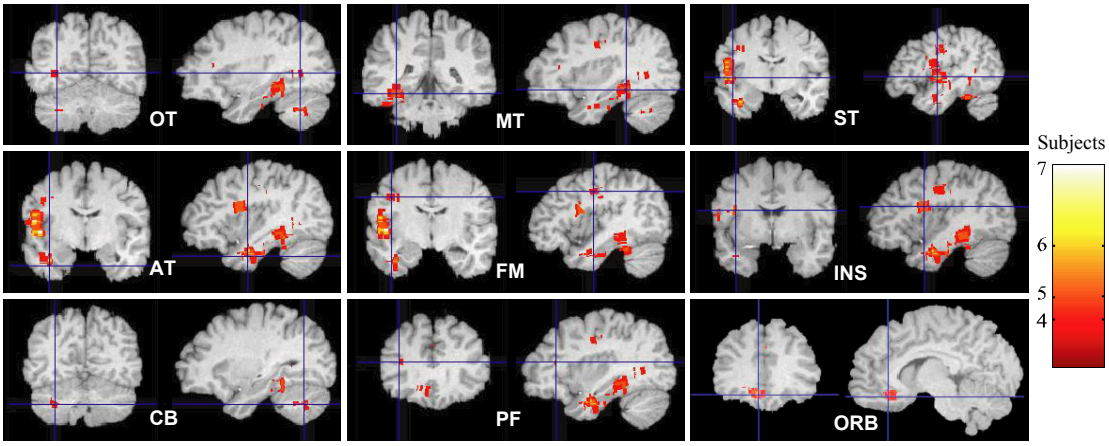

Figure 5.3: Systematically coherent areas across subjects during reading. Section overlays of brain areas in which the time courses of activation at 8-13 Hz were significantly coherent with those in other regions of the brain. This map represents intersubject consistency of spatial location of the nodes (color indicates number of subjects). Adapted from P5.

Characterization of interaction between the identified nodes was performed using SI and Granger causality. The SI analysis revealed differences between the experimental conditions, especially between isolated word reading and the other conditions (Fig. 5.4). Furthermore, phase coupling between the occipitotemporal cortex, superior temporal cortex and orbitofrontal cortex was stronger in conditions with faster rates of word presentation than in conditions with the slowest presentation rate. In addition, Granger causality analysis revealed that the information flow occurred predominantly from the posterior areas toward the anterior areas, and that the cerebellum and occipitotemporal cortex were the main driving nodes of the network.

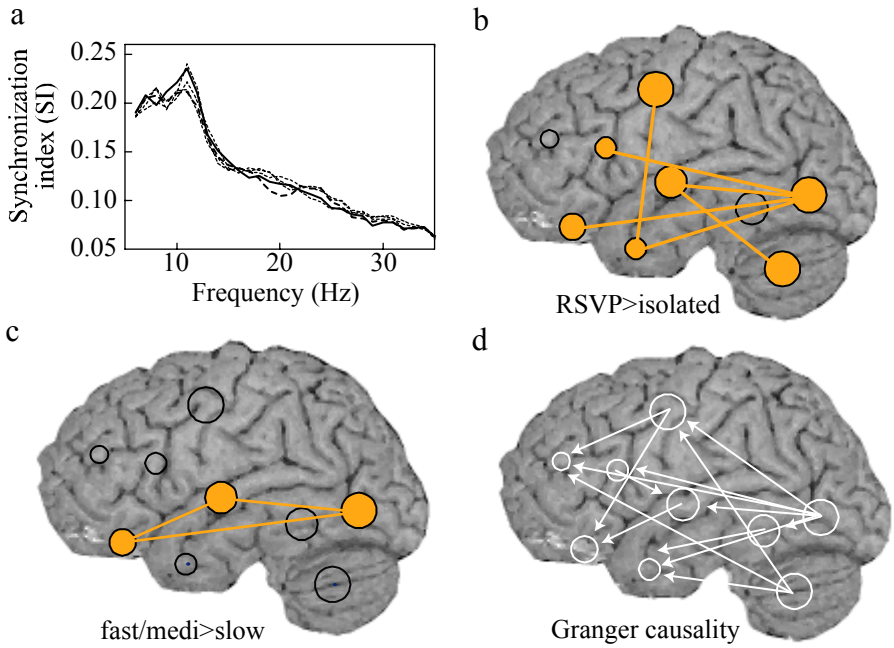

Figure 5.4: Characterization of the network behavior. a) SI as a function of frequency between occipitotemporal and orbitofrontal cortex for all five conditions in one subject. The fast RSVP task is shown with solid line (strongest SI), isolated words/nonwords condition with dashed line (weakest SI), and medium, slow, and scrambled conditions with thin dotted lines (in between). b) Connections for which SI was significantly higher in at least one RSVP condition than when reading isolated words/nonwords. c) Connections for which there was a significant effect of presentation rate on the SI (fast/medium > slow). d) Direction of information transfer (arrows), estimated using Granger causality and pooled over the RSVP conditions. The size of each nodal point indicates how many other nodes it was connected with. Adapted from P5.

5.3 Localization of activity versus cortico-cortical coupling (P6)

So far, the pattern of language function obtained from neuroimaging studies has been based on results from activation studies, i.e., from identifying areas which are more active during a language than a control task. However, according to current hypotheses, cognitive functions are based on connectivity within large-scale neuronal networks rather than on strictly localized processes (Mesulam, 1990; Varela et al., 2001). In some cases, connectivity has been evaluated between areas that have first been identified based on their activation (Weiss and Rappelsberger, 2000; Mormann et al., 2005). Still, the current understanding of language function is incomplete. It may well be that some of the areas involved in language processing do not show increased activation, but only increased coupling to other regions in the brain instead, and they would not be identified with activation measures nor included in the subsequent evaluation of connectivity. Thus, we compared how the picture obtained from the interaction analysis of reading (P5) relates to results obtained from existing language studies.

Based on our MEG connectivity analysis, areas that have been assigned specific roles during reading in neurophysiological activation studies, such as occipitotemporal cortex and superior temporal cortex, were perhaps the main nodes of the network. The occipitotemporal cortex (Fig. 5.5a) has been shown to be involved in letter-string analysis (Nobre and McCarthy, 1994; Tarkiainen et al., 1999) and the left superior temporal cortex (Fig. 5.5b) in reading comprehension (Helenius et al., 1998). In the connectivity analysis (Fig. 5.5d), Granger causality analysis revealed that the occipitotemporal cortex was the main driving node of the network. Thus, it appears that conversion from letter strings to words starting in occipitotemporal cortex feeds information to the rest of the network. Second, phase-coupling analysis revealed that both the occipitotemporal and superior temporal cortex were essential components in the process as the reading tasks became more demanding (Fig. 5.5c). Increased processing requirements were accompanied by stronger coupling between those areas.

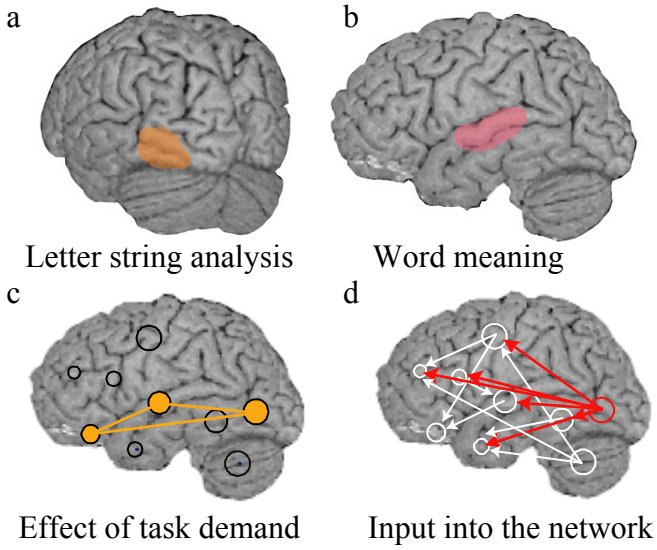

Figure 5.5: Areas found in MEG activation studies and connectivity studies of reading. Cortical areas involved in a) letter-string and b) word meaning analysis. c) Cortical areas whose coupling is modulated by the demand of the reading task. d) Input of information into the reading network. Adapted from P6.

Although hemodynamic and neurophysiological activation studies of language processing in the brain have yielded partly congruent results, there are also marked systematic differences, e.g., regarding areas involved in semantic processing. Intriguingly, the MEG connectivity analysis revealed a compilation of areas that encompasses many regions that have been observed either in hemodynamic or neurophysiological activation studies of speech comprehension, speech production and working memory (Nobre and McCarthy, 1995; Fiez and Petersen, 1998; Petrides et al., 2002). Connectivity analysis may thus capture elements that are differently detected by hemodynamic and neurophysiological measures of activation.

6 Conclusions and discussion

We developed new methods that enhance the analysis of cortical rhythmic activity and, above all, enable direct evaluation of rhythmic cortico-cortical interactions. Furthermore, through application of these methods to real recorded data, we were able to obtain new insights on cortical networks participating in both movement control and language processing.

The developed methods can be used to image rhythmic activity and its modulations in continuous and event-related tasks. Comparison with earlier methods showed that DICS is equally accurate and, in some cases, more sensitive in localizing oscillatory activity. Furthermore, DICS could better separate the activity of two nearby source areas. With the further development of erDICS, it is also possible to localize event-related modulation of rhythmic activity and, importantly, to evaluate its statistical significance. The main benefit of DICS is, however, that it enables both the imaging of coherence at the cortical level and the use of more complex measures in evaluating interactions between brain areas. Simulated data showed that DICS identified interacting areas accurately, and that the coherence estimate between them matched the true coherence under reasonable SNR conditions. Furthermore, the localization of the interacting areas is possible both using an external reference signal and by estimating the nodal points directly from the MEG data. Simulated data further showed that it was possible to identify the networks across subjects even when there was considerable intersubject variability in the location of the corresponding functional areas.

In addition, application of DICS to real data revealed interesting new information on both motor and language networks of the human brain. First, we found a substantial increase in phase synchronization between the motor and premotor cortices during Parkinsonian tremor. Second, in a slow finger movement task, we were able to identify the cortico-cortical network controlling the movements. Subsequent causal analysis between these areas uncovered the manner in which information flowed within this network. Third, when we applied the DICS approach to data recorded during continuous reading, we were able to identify interacting cortico-cortical networks systematically across subjects. Through the non-linear characterization of interactions within this network we found that the left superior temporal cortex and occipitotemporal cortex, in particular, are likely to play critical roles in reading. In addition, the medial temporal cortex and anterior temporal lobe areas participating specifically in comprehension were involved. Interestingly, the network also included areas that have been associated with language production rather than perception, and areas that have been reported not in language studies specifically but in visual recognition and working memory studies. The connectivity analysis thus indicated that language processing is wider-ranging than usually observed in activation studies of reading.

Subsequently, DICS has been further applied to a number of studies, ranging from motor control and motor learning to attention (Gross et al., 2004; Butz et al., 2006; Kessler et al., 2006; Pollok et al., 2006; Pollok et al., 2007). Thus, through DICS, it has become possible to identify areas based on their interaction with a cortical reference

area, and to quantify connectivity within the identified cortical networks. Although with MEG it not possible to achieve the spatial resolution and accuracy of fMRI, the source-level estimates obtained with DICS offer a substantial improvement to spatial specificity compared to EEG/MEG sensor-level connectivity analyses. Furthermore, as direct intracranial recordings are generally impossible, neurophysiological imaging provides the only direct window to the millisecond time-scale phenomena and frequency content of neural connectivity. The methods and techniques developed in this thesis can readily be applied by other researchers to investigate human brain function, at least with regards to localization of oscillatory power and connectivity analysis starting from an external reference signal. The former approach has recently been used by other groups in a number of studies relating to, e.g., action observation (Koelewijn et al., 2008) and memory processes (Osipova et al., 2006; Jokisch and Jensen, 2007). Thus, although the neuroscience results obtained with the methods developed in this thesis are yet limited in number, investigations using these approaches are becoming more systematic, revealing valuable new information of the human neural system.

Limitations and future topics

There are certain basic premises in DICS analysis. First, DICS relies on activation or instantaneous coupling measures in identifying the areas of interest. Causal interactions between nodal points can be analyzed afterwards. Thus, cortical areas that cannot be identified based on oscillatory power and whose mutual interaction is solely directional would be missed. Second, when the network has been identified, phase-coupling analysis can be performed between multiple frequencies, but the initial localization of coherent areas is performed within one frequency band. Local computation occurring at higher frequencies has been suggested to relate to integrative processing at specific phases of lower frequency oscillations (Jensen and Colgin, 2007). If this is the case, DICS analysis may fail to reveal areas that are fundamental in task performance. Third, DICS/erDICS analyses done in this thesis were based on wavelet and Fourier transformations. It has been proposed, however, that, e.g., gamma band activity is too widely spread in frequency to be detected with these methods (Hoogenboom et al., 2006; Gross et al., 2007).

These possible problems can be solved by incorporating new aspects into the methods. For example, causality can be used as a measure of interaction already at the stage of identifying the network nodes, not only as a measure for quantifying network behavior. This can be done by first obtaining an estimate of time-series of activity at all possible locations in the brain, and by evaluating causality between them. Similarly, cross-frequency coupling could be used already in the identification of areas of interest, either by performing phase-coupling analysis between multiple frequencies for the estimated time-series of activity at all cortical locations, or by estimating linear dependencies between different frequencies in the cross-spectral density matrix that is used in beamforming. Localization of wide-band activity could be enabled by using multi-tapers to estimate the cross spectral density matrix representing the sensor level data. This has been done successfully in analysis of gamma-band oscillations induced by visual stimuli (Hoogenboom et al., 2006).

DICS methodology can be developed further by also implementing changes that could, at least potentially, make the obtained results more accurate. Since the MEG signals are known to arise primarily from the pyramidal cells of the cortex, stricter anatomical constraints both in the location and orientation of the sources could benefit the DICS and erDICS estimates. Furthermore, higher-order covariance and higher-order source models have been suggested to yield more accurate localization of cortical activity than their lower-order counterparts (Huang et al., 2004; Jerbi et al., 2004). Similar improvements in the accuracy of the localization and characterization of cortical interactions could be important in identifying their functional role. The most important methodological issue regarding DICS is that it yields just one type of cortical level estimate of activity and connectivity, one that is based on spatial filtering, meaning that the estimates become invalid if perfectly correlated neural sources exist. An important validation of the techniques developed in this thesis would be to test whether estimates based on methods that are less sensitive to problems caused by highly correlated sources (e.g. the minimum-norm) would yield similar results.

Another important consideration is the type of sensors used in recording the data. The data presented in this thesis were collected with gradiometers. We also tested how inclusions of data recorded by magnetometers affected the obtained estimates; the results were essentially the same. Most likely, this lack of improvement resulted from the relatively noisy measurement environment. However, the Low Temperature Laboratory has since moved to new facilities, and the signal-to-noise ratio in the new measurement environment appears to have improved substantially. This change, combined with advanced noise cancellation techniques, such as the Signal Space Separation (SSS; Taulu et al., 2004; Taulu and Simola, 2006), should render magnetometers more beneficial in the analysis, especially regarding deep source areas. Furthermore, the DICS spatial resolution has been quantified for the Neuromag-122 system (P3) and should also be evaluated for the Vectorview™ system (both for the gradiometers and for all sensors), as well as other commonly used MEG systems and sensor types. Other groups have applied DICS successfully to, e.g., axial gradiometer data (Osipova et al., 2006; Jokisch and Jensen, 2007), but only for analysis of oscillatory power. In coherence analysis, the resolution of the estimates is even more critical than in analysis of rhythmic activity, and the spatial resolution of different types of neuromagnetometers in the different brain areas deserves careful investigation. Moreover, there is no theoretical reason why these methods could not be applied to EEG data as well. The only difference compared with MEG is that EEG analysis requires more careful modeling of the conductance of the human brain and skull. Application of DICS to EEG data would obviously make the presented approaches available to a much larger community of researchers. However, it would also be interesting to test whether combined use of EEG and MEG would make connectivity analysis more accurate, similar to what has been observed for combined use of EEG and MEG in analysis of cortical activation (Baillet et al., 1999; Sharon et al., 2007).

The most important topics for future research, however, relate to the application of DICS to real recorded data. First, recent findings have suggested that oscillatory activity is the component of neurophysiological activity which is most strongly correlated with hemodynamic responses (Logothetis et al., 2001; Mizuhara et al., 2004; de Munck et al., 2007). In humans, these correlations have so far been mostly estimated

between sensor-level EEG data and hemodynamic responses in specific cortical areas, without accurate information on the spatial distribution of the electric activity. Here, identification and quantification of activity in specific areas, obtainable with erDICS, could yield a clearer understanding of how the different modalities link to each other. Furthermore, fMRI and EEG have been found to show similar changes of interareal correlations during anesthesia (Lu et al., 2007). Interestingly, low-frequency band EEG correlations matched the coupling seen with fMRI, as opposed to the previously reported correlation of high-frequency band activity with fMRI (Logothetis et al., 2001). Thus, investigation of connectivity in the same task/paradigm with fMRI and DICS (using either EEG or MEG) should reveal how neural interactions at different frequencies relate to the coupling detected with hemodynamic measures. Second, we have seen for both motor and language networks that comparable areas are both active and connected during task performance. However, whether these areas are precisely the same, or whether there are systematic differences in their locations, is currently not known. In addition, it still remains open how specific the identified interacting networks are to the task performance, and how the interactions within the networks are modulated across a variety of tasks. Answers to these questions, obtainable with erDICS/DICS analyses of real recorded data, would substantially advance our understanding of the relationship between cortical information processing detected across imaging modalities, and of how cortical activations and interactions organize the vast amount of information the brain possesses into a single adaptable dynamic system.

Bibliography

Achard S, Salvador R, Whitcher B, Suckling J, Bullmore E. 2006. A resilient, low-frequency, small-world human brain functional network with highly connected association cortical hubs. J Neurosci 26, 63-72.

Ahonen AI, Hämäläinen MS, Ilmoniemi RJ, Kajola MJ, Knuutila JE, Simola JT, Vilkman VA. 1993. Sampling theory for neuromagnetic detector arrays. IEEE Trans Biomed Eng 40, 859-869.

Ahveninen J, Jääskelainen IP, Raij T, Bonmassar G, Devore S, Hämäläinen M, Levänen S, Lin FH, Sams M, Shinn-Cunningham BG, Witzel T, Belliveau JW. 2006. Task-modulated "what" and "where" pathways in human auditory cortex. Proc Natl Acad Sci USA 103, 14608-14613.

Aminoff MJ. 1986. Electroencephalography: general principles and clinical applications. In: Aminoff MJ, editor. Electrodiagnosis in Clinical Neurology. New York: Churchill Livingstone Inc. p 21-30.

Andres FG, Mima T, Schulman AE, Dichgans J, Hallett M, Gerloff C. 1999. Functional coupling of human cortical sensorimotor areas during bimanual skill acquisition. Brain 122, 855-870.

Astolfi L, Cincotti F, Babiloni C, Carducci F, Basilisco A, Rossini PM, Salinari S, Mattia D, Cerutti S, Dayan DB, Ding L, Ni Y, He B, Babiloni F. 2005a. Estimation of the cortical connectivity by high-resolution EEG and structural equation modeling: simulations and application to finger tapping data. IEEE Trans Biomed Eng 52, 757-768.

Astolfi L, Cincotti F, Mattia D, Babiloni C, Carducci F, Basilisco A, Rossini PM, Salinari S, Ding L, Ni Y, He B, Babiloni F. 2005b. Assessing cortical functional connectivity by linear inverse estimation and directed transfer function: simulations and application to real data. Clin Neurophysiol 116, 920-932.

Astolfi L, Cincotti F, Mattia D, Marciani MG, Baccala LA, de Vico Fallani F, Salinari S, Ursino M, Zavaglia M, Ding L, Edgar JC, Miller GA, He B, Babiloni F. 2007. Comparison of different cortical connectivity estimators for high-resolution EEG recordings. Hum Brain Mapp 28, 143-157.

Babiloni F, Cincotti F, Babiloni C, Carducci F, Mattia D, Astolfi L, Basilisco A, Rossini PM, Ding L, Ni Y, Cheng J, Christine K, Sweeney J, He B. 2005. Estimation of the cortical functional connectivity with the multimodal integration of high-resolution EEG and fMRI data by directed transfer function. Neuroimage 24, 118-131.

Baccala LA, Sameshima K. 2001. Partial directed coherence: a new concept in neural structure determination. Biol Cybern 84, 463-474.

Baillet S, Garnero L, Marin G, Hugonin JP. 1999. Combined MEG and EEG source imaging by minimization of mutual information. IEEE Trans Biomed Eng 46, 522-534.

Baillet S, Mosher C, Leahy M. 2001. Electromagnetic brain mapping. IEEE Signal processing magazine 18, 14-30.

Basser PJ, Mattiello J, LeBihan D. 1994a. Estimation of the effective self-diffusion tensor from the NMR spin echo. J Magn Reson B 103, 247-254.

Basser PJ, Mattiello J, LeBihan D. 1994b. MR diffusion tensor spectroscopy and imaging. Biophys J 66, 259-267.

Belliveau JW, Kennedy DN, Jr., McKinstry RC, Buchbinder BR, Weisskoff RM, Cohen MS, Vevea JM, Brady TJ, Rosen BR. 1991. Functional mapping of the human visual cortex by magnetic resonance imaging. Science 254, 716-719.

Berger H. 1929. Über das Elektroenkephalogramm des Menschen. Arch Psychiatr Nervenkr 87, 527-570.

Berger H. 1930. Über das Elektroenkephalogramm des Menschen II. J Psychol Neurol 40, 160-179.

Bragin A, Jando G, Nadasdy Z, Hetke J, Wise K, Buzsaki G. 1995. Gamma (40-100 Hz) oscillation in the hippocampus of the behaving rat. J Neurosci 15, 47-60.

Brenner D, Lipton J, Kaufman L, Williamson SJ. 1978. Somatically evoked magnetic fields of the human brain. Science 199, 81-83.

Brenner D, Williamson SJ, Kaufman L. 1975. Visually evoked magnetic fields of the human brain. Science 190, 480-482.

Brookes MJ, Stevenson CM, Barnes GR, Hillebrand A, Simpson MI, Francis ST, Morris PG. 2007. Beamformer reconstruction of correlated sources using a modified source model. Neuroimage 34, 1454-1465.

Butz M, Timmermann L, Gross J, Pollok B, Dirks M, Hefter H, Schnitzler A. 2006. Oscillatory coupling in writing and writer's cramp. J Physiol Paris 99, 14-20.

Buzsaki G, Buhl DL, Harris KD, Csicsvari J, Czeh B, Morozov A. 2003. Hippocampal network patterns of activity in the mouse. Neuroscience 116, 201-211.

Büchel C, Friston KJ. 1997. Modulation of connectivity in visual pathways by attention: cortical interactions evaluated with structural equation modelling and fMRI. Cereb Cortex 7, 768-778.

Büchel C, Friston KJ. 1998. Dynamic changes in effective connectivity characterized by variable parameter regression and Kalman filtering. Hum Brain Mapp 6, 403-408.

Canolty RT, Edwards E, Dalal SS, Soltani M, Nagarajan SS, Kirsch HE, Berger MS, Barbaro NM, Knight RT. 2006. High gamma power is phase-locked to theta oscillations in human neocortex. Science 313, 1626-1628.

Chatrian GE, Petersen MC, Lazarte JA. 1959. The blocking of the rolandic wicket rhythm and some central changes related to movement. Electroencephalogr Clin Neurophysiol Suppl 11, 497-510.

Chen Y, Bressler SL, Ding M. 2006. Frequency decomposition of conditional Granger causality and application to multivariate neural field potential data. J Neurosci Methods 150, 228-237.

Chrobak JJ, Buzsaki G. 1998. Gamma oscillations in the entorhinal cortex of the freely behaving rat. J Neurosci 18, 388-98.

Classen J, Gerloff C, Honda M, Hallett M. 1998. Integrative visuomotor behavior is associated with interregionally coherent oscillations in the human brain. J Neurophysiol 79, 1567-1573.

Cordes D, Haughton V, Carew JD, Arfanakis K, Maravilla K. 2002. Hierarchical clustering to measure connectivity in fMRI resting-state data. Magn Reson Imaging 20, 305-317.

Cosmelli D, David O, Lachaux JP, Martinerie J, Garnero L, Renault B, Varela F. 2004. Waves of consciousness: ongoing cortical patterns during binocular rivalry. Neuroimage 23, 128-140.

David O, Cosmelli D, Hasboun D, Garnero L. 2003. A multitrial analysis for revealing significant corticocortical networks in magnetoencephalography and electroencephalography. Neuroimage 20, 186-201.

David O, Garnero L, Cosmelli D, Varela FJ. 2002. Estimation of neural dynamics from MEG/EEG cortical current density maps: application to the reconstruction of large-scale cortical synchrony. IEEE Trans Biomed Eng 49, 975-987.

David O, Kilner JM, Friston KJ. 2006. Mechanisms of evoked and induced responses in MEG/EEG. Neuroimage 31, 1580-1591.

de Munck JC, Goncalves SI, Huijboom L, Kuijer JP, Pouwels PJ, Heethaar RM, Lopes da Silva FH. 2007. The hemodynamic response of the alpha rhythm: an EEG/fMRI study. Neuroimage 35, 1142-1151.

Dinse HR, Kruger K, Akhavan AC, Spengler F, Schoner G, Schreiner CE. 1997. Low-frequency oscillations of visual, auditory and somatosensory cortical neurons evoked by sensory stimulation. Int J Psychophysiol 26, 205-227.

Efron B. 1979. Bootstrap methods: another look at the jackknife. Ann Statistics 7, 1-26.

Eguiluz VM, Chialvo DR, Cecchi GA, Baliki M, Apkarian AV. 2005. Scale-free brain functional networks. Phys Rev Lett 94, 018102.

Engel AK, Kreiter AK, König P, Singer W. 1991. Synchronization of oscillatory neuronal responses between striate and extrastriate visual cortical areas of the cat. Proc Natl Acad Sci USA 88, 6048-6052.

Faes L, Pinna GD, Porta A, Maestri R, Nollo G. 2004. Surrogate data analysis for assessing the significance of the coherence function. IEEE Trans Biomed Eng 51, 1156-1166.

Fiez JA, Petersen SE. 1998. Neuroimaging studies of word reading. Proc Natl Acad Sci USA 95, 914-921.

Fox MD, Snyder AZ, Vincent JL, Corbetta M, Van Essen DC, Raichle ME. 2005. The human brain is intrinsically organized into dynamic, anticorrelated functional networks. Proc Natl Acad Sci USA 102, 9673-9678.

Freiwald WA, Valdes P, Bosch J, Biscay R, Jimenez JC, Rodriguez LM, Rodriguez V, Kreiter AK, Singer W. 1999. Testing non-linearity and directedness of interactions between neural groups in the macaque inferotemporal cortex. J Neurosci Methods 94, 105-119.

Friston K. 1994. Functional and Effective Connectivity in Neuroimaging: A Synthesis. Human Brain Mapping 2, 56-78.

Friston K, Frith CD, Frackowiak RS. 1993a. Time-dependent changes in effective connectivity measured with PET. Hum Brain Mapp 1, 69-80.

Friston KJ. 1997. Another neural code? Neuroimage 5, 213-220.

Friston KJ, Buchel C. 2000. Attentional modulation of effective connectivity from V2 to V5/MT in humans. Proc Natl Acad Sci USA 97, 7591-7596.

Friston KJ, Frith CD, Liddle PF, Frackowiak RS. 1993b. Functional connectivity: the principal-component analysis of large (PET) data sets. J Cereb Blood Flow Metab 13, 5-14.

Friston KJ, Harrison L, Penny W. 2003. Dynamic causal modelling. Neuroimage 19, 1273-1302.

Garrido MI, Kilner JM, Kiebel SJ, Friston KJ. 2007. Evoked brain responses are generated by feedback loops. Proc Natl Acad Sci USA 104, 20961-6.

Gastaut H. 1952. [Electrocorticographic study of the reactivity of rolandic rhythm.]. Rev Neurol (Paris) 87, 176-182.

Gavit L, Baillet S, Mangin JF, Pescatore J, Garnero L. 2001. A multiresolution framework to MEG/EEG source imaging. IEEE Trans Biomed Eng 48, 1080-1087.

Gerloff C, Richard J, Hadley J, Schulman AE, Honda M, Hallett M. 1998. Functional coupling and regional activation of human cortical motor areas during simple, internally paced and externally paced finger movements. Brain 121, 1513-1531.

Geweke J. 1982. Measurement of Linear Dependence and Feedback Between Multiple Time Series. Journal of the American Statistical Association 77, 304-313.

Geweke J. 1984. Measures of Conditional Linear Dependence and Feedback Between Time Series. Journal of the American Statistical Association 79, 907-915.

Gloor P, Ball G, Schaul N. 1977. Brain lesions that produce delta waves in the EEG. Neurology 27, 326-333.

Goebel R, Roebroeck A, Kim DS, Formisano E. 2003. Investigating directed cortical interactions in time-resolved fMRI data using vector autoregressive modeling and Granger causality mapping. Magn Reson Imaging 21, 1251-1261.

Granger CWJ. 1980. Testing for causality: a personal viewpoint. J Econ Dyn Control 2, 329-352.

Grasman RP, Huizenga HM, Waldorp LJ, Bocker KB, Molenaar PC. 2004. Frequency domain simultaneous source and source coherence estimation with an application to MEG. IEEE Trans Biomed Eng 51, 45-55.

Gray CM, Konig P, Engel AK, Singer W. 1989. Oscillatory responses in cat visual cortex exhibit inter-columnar synchronization which reflects global stimulus properties. Nature 338, 334-337.

Greicius MD, Krasnow B, Reiss AL, Menon V. 2003. Functional connectivity in the resting brain: a network analysis of the default mode hypothesis. Proc Natl Acad Sci USA 100, 253-258.

Greicius MD, Srivastava G, Reiss AL, Menon V. 2004. Default-mode network activity distinguishes Alzheimer's disease from healthy aging: evidence from functional MRI. Proc Natl Acad Sci USA 101, 4637-4642.

Grimm C, Schreiber A, Kristeva-Feige R, Mergner T, Hennig J, Lucking CH. 1998. A comparison between electric source localisation and fMRI during somatosensory stimulation. Electroencephalogr Clin Neurophysiol 106, 22-29.

Gross J, Ioannides AA. 1999. Linear transformations of data space in MEG. Phys Med Biol 44, 2081-2097.

Gross J, Schmitz F, Schnitzler I, Kessler K, Shapiro K, Hommel B, Schnitzler A. 2004. Modulation of long-range neural synchrony reflects temporal limitations of visual attention in humans. Proc Natl Acad Sci USA 101, 13050-13055.

Gross J, Schnitzler A, Timmermann L, Ploner M. 2007. Gamma oscillations in human primary somatosensory cortex reflect pain perception. PLoS Biol 5, e133.

Halliday DM, Rosenberg JR, Amjad AM, Breeze P, Conway BA, Farmer SF. 1995. A framework for the analysis of mixed time series/point process data--theory and application to the study of physiological tremor, single motor unit discharges and electromyograms. Prog Biophys Mol Biol 64, 237-278.

Hari R. 1991. On brain's magnetic responses to sensory stimuli. J Clin Neurophysiol 8, 157-169.

Hari R, Aittoniemi K, Järvinen ML, Katila T, Varpula T. 1980. Auditory evoked transient and sustained magnetic fields of the human brain. Localization of neural generators. Exp Brain Res 40, 237-240.

Hari R, Ilmoniemi RJ. 1986. Cerebral magnetic fields. Crit Rev Biomed Eng 14, 93-126.

Hari R, Salmelin R. 1997. Human cortical oscillations: a neuromagnetic view through the skull. Trends Neurosci 20, 44-49.

Helenius P, Salmelin R, Service E, Connolly JF. 1998. Distinct time courses of word and context comprehension in the left temporal cortex. Brain 121, 1133-1142.

Helmholz H. 1853. Ueber einige Gesetze der Vertheilung elektrischer Ströme in körperlichen Leitern, mit Anwendung auf die thierisch-elektrischen Versuche. Ann. Phsy. Chem. 89, 211-233, 353-377.

Herdman AT, Wollbrink A, Chau W, Ishii R, Ross B, Pantev C. 2003. Determination of activation areas in the human auditory cortex by means of synthetic aperture magnetometry. Neuroimage 20, 995-1005.

Hillebrand A, Singh KD, Holliday IE, Furlong PL, Barnes GR. 2005. A new approach to neuroimaging with magnetoencephalography. Hum Brain Mapp 25, 199-211.

Hoogenboom N, Schoffelen JM, Oostenveld R, Parkes LM, Fries P. 2006. Localizing human visual gamma-band activity in frequency, time and space. Neuroimage 29, 764-773.

Horwitz B, Warner B, Fitzer J, Tagamets MA, Husain FT, Long TW. 2005. Investigating the neural basis for functional and effective connectivity. Application to fMRI. Philos Trans R Soc Lond B Biol Sci 360, 1093-1108.

Huang MX, Shih JJ, Lee RR, Harrington DL, Thoma RJ, Weisend MP, Hanlon F, Paulson KM, Li T, Martin K, Millers GA, Canive JM. 2004. Commonalities and differences among vectorized beamformers in electromagnetic source imaging. Brain Topogr 16, 139-158.

Hämäläinen M, Hari R, Ilmoniemi RJ, Knuutila J, Lounasmaa OV. 1993. Magnetoencephalography — theory, instrumentation, and applications to noninvasive studies of the working human brain. Rev Mod Phys 65, 413-497.

Hämäläinen MS, Ilmoniemi RJ. 1984. Interpreting measured magnetic fields of the brain: Estiamtes of current distributions. Helsinki University of Technology, Finland. Report nr TKK-F-A559.

Hämäläinen MS, Sarvas J. 1989. Realistic conductivity geometry model of the human head for interpretation of neuromagnetic data. IEEE Trans Biomed Eng 36, 165-171.

Ilmoniemi RJ, Virtanen J, Ruohonen J, Karhu J, Aronen HJ, Naatanen R, Katila T. 1997. Neuronal responses to magnetic stimulation reveal cortical reactivity and connectivity. Neuroreport 8, 3537-40.

Ioannides AA, Liu LC, Kwapien J, Drozdz S, Streit M. 2000. Coupling of regional activations in a human brain during an object and face affect recognition task. Hum Brain Mapp 11, 77-92.

Ishii R, Shinosaki K, Ukai S, Inouye T, Ishihara T, Yoshimine T, Hirabuki N, Asada H, Kihara T, Robinson SE, Takeda M. 1999. Medial prefrontal cortex generates frontal midline theta rhythm. Neuroreport 10, 675-679.

Ivry RB. 1996. The representation of temporal information in perception and motor control. Curr Opin Neurobiol 6, 851-857.

Jensen O, Colgin LL. 2007. Cross-frequency coupling between neuronal oscillations. Trends Cogn Sci 11, 267-269.

Jensen O, Gelfand J, Kounios J, Lisman JE. 2002. Oscillations in the alpha band (9-12 Hz) increase with memory load during retention in a short-term memory task. Cereb Cortex 12, 877-882.

Jensen O, Tesche CD. 2002. Frontal theta activity in humans increases with memory load in a working memory task. Eur J Neurosci 15, 1395-1399.

Jensen O, Vanni S. 2002. A new method to identify multiple sources of oscillatory activity from magnetoencephalographic data. Neuroimage 15, 568-574.

Jerbi K, Baillet S, Mosher JC, Nolte G, Garnero L, Leahy RM. 2004. Localization of realistic cortical activity in MEG using current multipoles. Neuroimage 22, 779-793.

Jerbi K, Lachaux JP, N'Diaye K, Pantazis D, Leahy RM, Garnero L, Baillet S. 2007. Coherent neural representation of hand speed in humans revealed by MEG imaging. Proc Natl Acad Sci USA 104, 7676-7681.

Jokisch D, Jensen O. 2007. Modulation of gamma and alpha activity during a working memory task engaging the dorsal or ventral stream. J Neurosci 27, 3244-51.

Kaiser J, Bühler M, Lutzenberger W. 2004. Magnetoencephalographic gamma-band responses to illusory triangles in humans. Neuroimage 23, 551-560.

Kaminski M, Ding M, Truccolo WA, Bressler SL. 2001. Evaluating causal relations in neural systems: granger causality, directed transfer function and statistical assessment of significance. Biol Cybern 85, 145-157.

Kaufman L, Okada Y, Brenner D, Williamson SJ. 1981. On the relation between somatic evoked potentials and fields. Int J Neurosci 15, 223-239.

Kaufman L, Schwartz B, Salustri C, Williamson SJ. 1990. Modulation of spontaneous brain activity during mental imagery. J Cogn Neurosci 2, 124-132.

Kaukoranta E, Hämäläinen M, Sarvas J, Hari R. 1986. Mixed and sensory nerve stimulations activate different cytoarchitectonic areas in the human primary somatosensory cortex SI. Neuromagnetic recordings and statistical considerations. Exp Brain Res 63, 60-66.

Kessler K, Biermann-Ruben K, Jonas M, Siebner HR, Bäumer T, Münchau A, Schnitzler A. 2006. Investigating the human mirror neuron system by means of cortical synchronization during the imitation of biological movements. Neuroimage 33, 227-238.

Kiebel SJ, Garrido MI, Friston KJ. 2007. Dynamic causal modelling of evoked responses: the role of intrinsic connections. Neuroimage 36, 332-45.

Kim DS, Ronen I, Olman C, Kim SG, Ugurbil K, Toth LJ. 2004. Spatial relationship between neuronal activity and BOLD functional MRI. Neuroimage 21, 876-885.

Koelewijn T, van Schie HT, Bekkering H, Oostenveld R, Jensen O. 2008. Motor-cortical beta oscillations are modulated by correctness of observed action. Neuroimage 40, 767-775.

Komssi S, Aronen HJ, Huttunen J, Kesaniemi M, Soinne L, Nikouline VV, Ollikainen M, Roine RO, Karhu J, Savolainen S, Ilmoniemi RJ. 2002. Ipsi- and contralateral EEG reactions to transcranial magnetic stimulation. Clin Neurophysiol 113, 175-84.

Kopell N, Ermentrout GB, Whittington MA, Traub RD. 2000. Gamma rhythms and beta rhythms have different synchronization properties. Proc Nat Acad Sci Usa 97, 1867-1872.

König P, Engel AK. 1995. Correlated firing in sensory-motor systems. Curr Opin Neurobiol 5, 511-519.

La Berge D. 1995. Attentional processing. Cambridge, MA: Harvard University Press.

Lachaux JP, Rodriguez E, Martinerie J, Varela FJ. 1999. Measuring phase synchrony in brain signals. Hum Brain Mapp 8, 194-208.

Lahaye PJ, Poline JB, Flandin G, Dodel S, Garnero L. 2003. Functional connectivity: studying nonlinear, delayed interactions between BOLD signals. Neuroimage 20, 962-974.

Laufs H, Kleinschmidt A, Beyerle A, Eger E, Salek-Haddadi A, Preibisch C, Krakow K. 2003. EEG-correlated fMRI of human alpha activity. Neuroimage 19, 1463-1476.

Llinás RR. 1988. The intrinsic electrophysiological properties of mammalian neurons: insights into central nervous system function. Science 242, 1654-1664.

Logothetis NK, Pauls J, Augath M, Trinath T, Oeltermann A. 2001. Neurophysiological investigation of the basis of the fMRI signal. Nature 412, 150-157.

Lu H, Zuo Y, Gu H, Waltz JA, Zhan W, Scholl CA, Rea W, Yang Y, Stein EA. 2007. Synchronized delta oscillations correlate with the resting-state functional MRI signal. Proc Natl Acad Sci USA 104, 18265-18269.

Makeig S, Westerfield M, Jung TP, Enghoff S, Townsend J, Courchesne E, Sejnowski TJ. 2002. Dynamic brain sources of visual evoked responses. Science 295, 690-4.

Massimini M, Ferrarelli F, Huber R, Esser SK, Singh H, Tononi G. 2005. Breakdown of cortical effective connectivity during sleep. Science 309, 2228-32.

Matsuura K, Okabe Y. 1995. Selective minimum-norm solution of the biomagnetic inverse problem. IEEE Trans Biomed Eng 42, 608-615.

Mazaheri A, Jensen O. 2006. Posterior alpha activity is not phase-reset by visual stimuli. Proc Natl Acad Sci USA 103, 2948-2952.

McIntosh AR, Gonzalez-Lima F. 1991. Structural modeling of functional neural pathways mapped with 2-deoxyglucose: effects of acoustic startle habituation on the auditory system. Brain Res 547, 295-302.

McIntosh AR, Gonzalez-Lima F. 1994. Structural Equation Modeling and its application to Network Analysis in Functional Brain Imaging. Hum Brain Mapp 2, 2-22.

Mechelli A, Price CJ, Friston KJ, Ishai A. 2004. Where bottom-up meets top-down: neuronal interactions during perception and imagery. Cereb Cortex 14, 1256-1265.

Medendorp WP, Kramer GF, Jensen O, Oostenveld R, Schoffelen JM, Fries P. 2006. Oscillatory Activity in Human Parietal and Occipital Cortex Shows Hemispheric Lateralization and Memory Effects in a Delayed Double-Step Saccade Task. Cereb Cortex 17, 2364-2674.

Menon V, Ford JM, Lim KO, Glover GH, Pfefferbaum A. 1997. Combined event-related fMRI and EEG evidence for temporal-parietal cortex activation during target detection. Neuroreport 8, 3029-3037.

Mesulam MM. 1990. Large-scale neurocognitive networks and distributed processing for attention, language, and memory. Ann Neurol 28, 597-613.

Miltner WH, Braun C, Arnold M, Witte H, Taub E. 1999. Coherence of gamma-band EEG activity as a basis for associative learning. Nature 397, 434-436.

Mizuhara H, Wang LQ, Kobayashi K, Yamaguchi Y. 2004. A long-range cortical network emerging with theta oscillation in a mental task. Neuroreport 15, 1233-1238.

Mori S, Van Zijl PC. 2002. Fiber tracking: principles and strategies - a technical review. NMR Biomed 15, 468-480.

Mormann F, Fell J, Axmacher N, Weber B, Lehnertz K, Elger CE, Fernandez G. 2005. Phase/amplitude reset and theta-gamma interaction in the human medial temporal lobe during a continuous word recognition memory task. Hippocampus 15, 890-900.

Mosher J, Baillet S, Leahy M. 2003. Equivalence of linear approaches in bioelectromagnetic inverse solutions. IEEE Workshop on Statistical Signal Processing 294-297.

Mosher J, Leahy M. 1999. Source Localization Using Recursively Applied and Projected (RAP) MUSIC. IEEE Transactions on signal processing 47, 332-340.

Mosher JC, Lewis PS, Leahy RM. 1992. Multiple dipole modeling and localization from spatio-temporal MEG data. IEEE Trans Biomed Eng 39, 541-557.

Mulert C, Jäger L, Schmitt R, Bussfeld P, Pogarell O, Möller HJ, Juckel G, Hegerl U. 2004. Integration of fMRI and simultaneous EEG: towards a comprehensive understanding of localization and time-course of brain activity in target detection. Neuroimage 22, 83-94.

Murthy VN, Fetz EE. 1992. Coherent 25- to 35-Hz oscillations in the sensorimotor cortex of awake behaving monkeys. Proc Natl Acad Sci U S A 89, 5670-5674.

Mäkelä JP, Hari P, Karhu J, Salmelin R, Teräväinen H. 1993. Suppression of magnetic mu rhythm during parkinsonian tremor. Brain Res 617, 189-193.

Nobre AC, Allison T, McCarthy G. 1994. Word recognition in the human inferior temporal lobe. Nature 372, 260-263.

Nobre AC, McCarthy G. 1994. Language-related ERPs: scalp distributions and modulation by word type and semantic priming. J Cogn Neurosci 6, 233-255.

Nobre AC, McCarthy G. 1995. Language-related field potentials in the anterior-medial temporal lobe: II. Effects of word type and semantic priming. J Neurosci 15, 1090-1098.

Ogawa S, Tank DW, Menon R, Ellermann JM, Kim SG, Merkle H, Ugurbil K. 1992. Intrinsic signal changes accompanying sensory stimulation: functional brain mapping with magnetic resonance imaging. Proc Natl Acad Sci USA 89, 5951-5955.

Oishi N, Mima T, Ishii K, Bushara KO, Hiraoka T, Ueki Y, Fukuyama H, Hallett M. 2007. Neural correlates of regional EEG power change. Neuroimage 36, 1301-1312.

Okada YC, Wu J, Kyuhou S. 1997. Genesis of MEG signals in a mammalian CNS structure. Electroencephalogr Clin Neurophysiol 103, 474-485.

Osipova D, Takashima A, Oostenveld R, Fernandez G, Maris E, Jensen O. 2006. Theta and gamma oscillations predict encoding and retrieval of declarative memory. J Neurosci 26, 7523-7531.

Palus M, Hoyer D. 1998. Detecting nonlinearity and phase synchronization with surrogate data. IEEE Eng Med Biol Mag 17, 40-45.

Palva JM, Palva S, Kaila K. 2005. Phase synchrony among neuronal oscillations in the human cortex. J Neurosci 25, 3962-3972.

Parker GJ, Luzzi S, Alexander DC, Wheeler-Kingshott CA, Ciccarelli O, Lambon Ralph MA. 2005. Lateralization of ventral and dorsal auditory-language pathways in the human brain. Neuroimage 24, 656-666.

Penfield W. 1954. Mechanisms of voluntary movement. Brain 77, 1-17.

Penny WD, Kiebel SJ, Kilner JM, Rugg MD. 2002. Event-related brain dynamics. Trends Neurosci 25, 387-9.

Penny WD, Stephan KE, Mechelli A, Friston KJ. 2004. Modelling functional integration: a comparison of structural equation and dynamic causal models. Neuroimage 23 Suppl 1, S264-S274.

Petrides M, Alivisatos B, Frey S. 2002. Differential activation of the human orbital, mid-ventrolateral, and mid-dorsolateral prefrontal cortex during the processing of visual stimuli. Proc Natl Acad Sci USA 99, 5649-5654.

Pfurtscheller G. 1977. Graphical display and statistical evaluation of event-related desynchronization (ERD). Electroencephalogr Clin Neurophysiol 43, 757-760.

Pfurtscheller G. 1981. Central beta rhythm during sensorimotor activities in man. Electroencephalogr Clin Neurophysiol 51, 253-264.

Pfurtscheller G. 1992. Event-related synchronization (ERS): an electrophysiological correlate of cortical areas at rest. Electroencephalogr Clin Neurophysiol 83, 62-69.

Pfurtscheller G, Lopes da Silva FH. 1999. Event-related EEG/MEG synchronization and desynchronization: basic principles. Clin Neurophysiol 110, 1842-1857.

Pfurtscheller G, Neuper C, Pichler-Zalaudek K, Edlinger G, Lopes da Silva FH. 2000. Do brain oscillations of different frequencies indicate interaction between cortical areas in humans? Neurosci Lett 286, 66-68.

Ploner M, Gross J, Timmermann L, Pollok B, Schnitzler A. 2006. Oscillatory activity reflects the excitability of the human somatosensory system. Neuroimage 32, 1231-1236.

Pollok B, Butz M, Gross J, Schnitzler A. 2007. Intercerebellar coupling contributes to bimanual coordination. J Cogn Neurosci 19, 704-719.

Pollok B, Gross J, Schnitzler A. 2006. Asymmetry of interhemispheric interaction in left-handed subjects. Exp Brain Res 175, 268-275.

Price CJ, Wise RJS, Watson JDG, Patterson K, Howard D, Frackowiak RSJ. 1994. Brain activity during reading. The effects of exposure duration and task. Brain 117, 1255-1269.

Raichle ME, MacLeod AM, Snyder AZ, Powers WJ, Gusnard DA, Shulman GL. 2001. A default mode of brain function. Proc Natl Acad Sci USA 98, 676-682.

Robinson SE, Vrba J. Functional neuroimaging by Synthetic Aperture Magnetometry (SAM). In: Yoshimoto T, Kotani M, Kuriki S, Karibe H, Nakasato B, editors. Recent Advances in Biomagnetism; 1997; Sendai. Tohoku University Press, Sendai. p 302-305.

Rodriguez E, George N, Lachaux JP, Martinerie J, Renault B, Varela FJ. 1999. Perception's shadow: long-distance synchronization of human brain activity. Nature 397, 430-433.

Roebroeck A, Formisano E, Goebel R. 2005. Mapping directed influence over the brain using Granger causality and fMRI. Neuroimage 25, 230-242.

Roelfsema PR, Engel AK, König P, Singer W. 1997. Visuomotor integration is associated with zero time-lag synchronization among cortical areas. Nature 385, 157-161.

Rosenblum MG, Pikovsky AS. 2001. Detecting direction of coupling in interacting oscillators. Phys Rev E Stat Nonlin Soft Matter Phys 64, 045202.

Saarinen T, Laaksonen H, Parviainen T, Salmelin R. 2006. Motor cortex dynamics in visuomotor production of speech and non-speech mouth movements. Cereb Cortex 16, 212-222.

Salenius S, Kajola M, Thompson WL, Kosslyn S, Hari R. 1995. Reactivity of magnetic parieto-occipital alpha rhythm during visual imagery. Electroencephalogr Clin Neurophysiol 95, 453-462.

Salmelin R, Hari R. 1994a. Characterization of spontaneous MEG rhythms in healthy adults. Electroencephalogr Clin Neurophysiol 91, 237-248.

Salmelin R, Hari R. 1994b. Spatiotemporal characteristics of sensorimotor neuromagnetic rhythms related to thumb movement. Neuroscience 60, 537-550.

Salmelin R, Hari R, Lounasmaa OV, Sams M. 1994. Dynamics of brain activation during picture naming. Nature 368, 463-465.

Salmelin R, Hämäläinen M, Kajola M, Hari R. 1995. Functional segregation of movement-related rhythmic activity in the human brain. Neuroimage 2, 237-243.

Salmelin RH, Hämäläinen MS. 1995. Dipole modelling of MEG rhythms in time and frequency domains. Brain Topogr 7, 251-257.

Sameshima K, Baccala LA. 1999. Using partial directed coherence to describe neuronal ensemble interactions. J Neurosci Methods 94, 93-103.

Sarnthein J, Petsche H, Rappelsberger P, Shaw GL, von Stein A. 1998. Synchronization between prefrontal and posterior association cortex during human working memory. Proc Natl Acad Sci USA 95, 7092-7096.

Sarvas J. 1987. Basic mathematical and electromagnetic concepts of the biomagnetic inverse problem. Phys Med Biol 32, 11-22.

Schack B, Vath N, Petsche H, Geissler HG, Möller E. 2002. Phase-coupling of theta-gamma EEG rhythms during short-term memory processing. Int J Psychophysiol 44, 143-163.

Scherg M, Hari R, Hämäläinen M. 1989. Frequency-specific sources of the auditory N19-P30-P50 response detected by a multiple source analysis of evoked magnetic fields and potentials. In: Williamson SJ, Hoke M, Stroink G, Kotani M, editors. Advances in Biomagnetism. New York: Plenum. p 97-100.

Schreiber T, Schmitz A. 2000. Surrogate time series. Physica D 142, 346-82.

Sekihara K, Nagarajan SS, Poeppel D, Marantz A, Miyashita Y. 2001. Reconstructing spatio-temporal activities of neural sources using an MEG vector beamformer technique. IEEE Trans Biomed Eng 48, 760-771.

Shah AS, Bressler SL, Knuth KH, Ding M, Mehta AD, Ulbert I, Schroeder CE. 2004. Neural dynamics and the fundamental mechanisms of event-related brain potentials. Cereb Cortex 14, 476-83.

Sharon D, Hamalainen MS, Tootell RB, Halgren E, Belliveau JW. 2007. The advantage of combining MEG and EEG: Comparison to fMRI in focally stimulated visual cortex. Neuroimage.

Simões C, Jensen O, Parkkonen L, Hari R. 2003. Phase locking between human primary and secondary somatosensory cortices. Proc Natl Acad Sci USA 100, 2691-2694.

Singer W. 1993. Synchronization of cortical activity and its putative role in information processing and learning. Annu Rev Physiol 55, 349-374.

Singer W. 1999. Neuronal synchrony: a versatile code for the definition of relations? Neuron 24, 49-65.

Singer W, Gray CM. 1995. Visual feature integration and the temporal correlation hypothesis. Annu Rev Neurosci 18, 555-586.

Singh KD, Barnes GR, Hillebrand A. 2003. Group imaging of task-related changes in cortical synchronisation using nonparametric permutation testing. Neuroimage 19, 1589-1601.

Steriade M, Gloor P, Llinás RR, Lopes da Silva FH, Mesulam M-M. 1990. Basic mechanisms of cerebral rhythmic activities. Electroenceph Clin Neurophysiol 76, 481-508.

Steriade M, Llinás RR. 1988. The functional states of the thalamus and the associated neuronal interplay. Physiol Review 68, 649-742.

Tallon-Baudry C, Bertrand O, Delpuech C, Permier J. 1997. Oscillatory gamma-band (30-70 Hz) activity induced by a visual search task in humans. J Neurosci 17, 722-734.

Tallon-Baudry C, Bertrand O, Fischer C. 2001. Oscillatory synchrony between human extrastriate areas during visual short-term memory maintenance. J Neurosci 21, RC177.

Tarkiainen A, Helenius P, Hansen PC, Cornelissen PL, Salmelin R. 1999. Dynamics of letter string perception in the human occipitotemporal cortex. Brain 122, 2119-2132.

Tarkiainen A, Liljeström M, Seppä M, Salmelin R. 2003. The 3D topography of MEG source localization accuracy: effects of conductor model and noise. Clin Neurophysiol 114, 1977-1992.

Tass P, Rosenblum M, Weule J, Kurths J, Pikovsky A, Volkmann J, Schnitzler A, Freund H-J. 1998. Detection of n:m phase locking from noisy data: application to magnetoencephalography. Phys Rev Lett 81, 3291-3294.

Taulu S, Kajola M, Simola J. 2004. Suppression of interference and artifacts by the Signal Space Separation Method. Brain Topogr 16, 269-75.

Taulu S, Simola J. 2006. Spatiotemporal signal space separation method for rejecting nearby interference in MEG measurements. Phys Med Biol 51, 1759-68.

Ter-Pogossian MM, Phelps ME, Hoffman EJ, Mullani NA. 1975. A positron-emission transaxial tomograph for nuclear imaging (PETT). Radiology 114, 89-98.

Tiihonen J, Hari R, Kajola M, Karhu J, Ahlfors S, Tissari S. 1991. Magnetoencephalographic 10-Hz rhythm from the human auditory cortex. Neurosci Lett 129, 303-305.

Toosy AT, Ciccarelli O, Parker GJ, Wheeler-Kingshott CA, Miller DH, Thompson AJ. 2004. Characterizing function-structure relationships in the human visual system with functional MRI and diffusion tensor imaging. Neuroimage 21, 1452-1463.

Tuomisto T, Hari R, Katila T, Poutanen T, Varpula T. 1983. Studies of auditory evoked magnetic and electric responses: Modality specificity and modelling. Nuovo Cimento D 2, 471-483.

Uutela K, Hämäläinen M, Somersalo E. 1999. Visualization of magnetoencephalographic data using minimum current estimates. Neuroimage 10, 173-180.

Vallbo AB, Wessberg J. 1993. Organization of motor output in slow finger movements in man. J Physiol 469, 673-691.

Van Veen BD, Buckley K. 1988. Beamforming: A Versatile Approach to Spatial Filtering. IEEE ASSP Magazine 5, 4-24.

Van Veen BD, van Drongelen W, Yuchtman M, Suzuki A. 1997. Localization of brain electrical activity via linearly constrained minimum variance spatial filtering. IEEE Trans Biomed Eng 44, 867-880.

Varela F, Lachaux JP, Rodriguez E, Martinerie J. 2001. The brainweb: phase synchronization and large-scale integration. Nat Rev Neurosci 2, 229-239.

Weiss S, Rappelsberger P. 2000. Long-range EEG synchronization during word encoding correlates with successful memory performance. Brain Res Cogn Brain Res 9, 299-312.

Welch P. 1967. The use of fast Fourier transform for the estimation of power spectra: A method based on time averaging over short, modified periodograms. IEEE Trans. Audio 15, 70-73.

Whittingstall K, Stroink G, Schmidt M. 2007. Evaluating the spatial relationship of event-related potential and functional MRI sources in the primary visual cortex. Hum Brain Mapp 28, 134-142.

Williams RW, Herrup K. 1988. The control of neuron number. Annu Rev Neurosci 11, 423-453.

von der Malsburg C. 1999. The what and why of binding: the modeler's perspective. Neuron 24, 95-104, 111-125.

von Stein A, Chiang C, König P. 2000. Top-down processing mediated by interareal synchronization. Proc Natl Acad Sci USA 97, 14748-14753.

von Stein A, Rappelsberger P, Sarnthein J, Petsche H. 1999. Synchronization between temporal and parietal cortex during multimodal object processing in man. Cereb Cortex 9, 137-150.

Vrba J, Robinson SE. 2001. Signal processing in magnetoencephalography. Methods 25, 249-271.

Xiong J, Rao S, Jerabek P, Zamarripa F, Woldorff M, Lancaster J, Fox PT. 2000. Intersubject variability in cortical activations during a complex language task. Neuroimage 12, 326-339.

Zimmerman JE, Silver AH. 1966. Macroscopic quantum interference effects through superconducting point contacts. Phys Rev 141, 367-375.

ISBN 978-951-22-9339-1
ISBN 978-951-22-9340-7 (PDF)
ISSN 1795-2239
ISSN 1795-4584 (PDF)